IOPscience iopscience.iop.org

Home Search Collections Journals About Contact us My IOPscience

Physical properties of RCo_2 Laves phases

This article has been downloaded from IOPscience. Please scroll down to see the full text article.

2001 J. Phys.: Condens. Matter 13 R385

(http://iopscience.iop.org/0953-8984/13/23/202)

View the table of contents for this issue, or go to the journal homepage for more

Download details:
IP Address: 171.66.16.226
The article was downloaded on 16/05/2010 at 13:28

Please note that terms and conditions apply.

INSTITUTE OF PHYSICS PUBLISHING JOURNAL OF PHYSICS: CONDENSED MATTER

J. Phys.: Condens. Matter **13** (2001) R385–R413 www.iop.org/Journals/cm PII: S0953-8984(01)22385-6

REVIEW ARTICLE

Physical properties of RCo_2 Laves phases

E Gratz[1] **and A S Markosyan**[2,3]

[1] Institute for Experimental Physics, Technical University Vienna, Wiedner Hauptstrasse 8–10, A-1040, Austria
[2] Faculty of Physics, M V Lomonosov Moscow State University, 119899 Moscow, Russia

E-mail: gratz@xphys.tuwien.ac.at and marko@plms.phys.msu.su

Received 1 March 2001, in final form 11 April 2001

Abstract

The large variety of magnetic phenomena observed in the Co based Laves phases are reviewed. Following the band structure calculations it is argued that the outstanding magnetic features of the RCo_2 intermetallics are intimately related to the position of the Fermi level, which is near to a local peak in $N(\varepsilon)$. This is why the Co 3d-electron system reacts sensitively either to the molecular field of the R partner element or to the changes of external parameters such as a magnetic field or pressure. Magnetic, magnetoelastic and transport measurements of RCo_2 compounds and related pseudobinaries such as $R(Co_{1-x}Al_x)_2$ with R either magnetic or nonmagnetic rare earth element are shown and discussed. The conditions for the appearance of itinerant electron metamagnetism and spin fluctuations are outlined. In particular, the influences of spin fluctuations on physical properties, e.g. the susceptibility, thermal expansion and transport phenomena, are demonstrated.

1. Introduction

For more than 20 years the cubic Laves phases RCo_2 have been a subject of particular interest in solid state physics. The main reason for this is that the RCo_2 series meets well the requirements one can wish for a *true model material*. Many phenomena observed in these intermetallics are determined mainly by one, or at least two, dominating mechanisms. This circumstance facilitates essentially the interpretation of their physical properties by the use of general and simple theoretical models. Therefore the concepts developed for the RCo_2 compounds can easily be used when considering other metallic systems.

Among the rare earth (R)–3d transition metal cubic Laves phases the magnetism of the 3d partner is most strongly influenced by the magnetic R sublattice in the RCo_2 series. Within this series, $ScCo_2$, YCo_2 and $LuCo_2$ are nonmagnetic, however showing features characteristic for exchange enhanced paramagnetism. The driving mechanism which determines the magnetic properties of these compounds rests upon an interplay (hybridization) of the Co 3d- and the

[3] Address for correspondence: A S Markosyan, Laboratory of Problems for Magnetism, Faculty of Physics, M V Lomonosov Moscow State University, 119899 Moscow, Russia.

 © 2001 IOP Publishing Ltd Printed in the UK

outside rare earth d-wave functions (3d–5d in $LuCo_2$, 3d–4d in YCo_2 and 3d–3d in $ScCo_2$). In the absence of an internal molecular field this hybridization is expected to be the dominant factor, forming most of their physical properties. The hybridization is also important in the paramagnetic state of the RCo_2 compounds with magnetic R elements.

In magnetic RCo_2 compounds the intersublattice f–d exchange field drives the Co sublattice into a ferromagnetic state, with the exception of $TmCo_2$ where the f–d exchange interaction does not reach the critical value of about 70 T. Owing to the negative sign of the f–d interaction, compounds with the light R elements are ferromagnetic (i.e., the sublattices are aligned parallel), whereas those with heavy R (Gd up to Er) are accordingly ferrimagnetic. The properties of these compounds (especially in their paramagnetic state) cannot satisfactorily be explained ignoring dynamic effects, such as spin fluctuations (SF). The influence of SF on the physical properties can most clearly be seen in dynamic measurements, such as the transport phenomena.

In order to separate and demonstrate the interplay among the different electronic subsystems (3d, 4d, 5d and 4f electrons), measurements of pseudobinary systems are performed, where either R or Co is replaced by another element. In few cases both, R and Co are simultaneously substituted. Although for many effects observed in the RCo_2 Laves phases plausible explanations have been found, not all of their properties are yet understood.

The aim of the present publication is to show and discuss appropriate selected examples of those Co based Laves phases which might be useful for the understanding of further investigations of more complex magnetic intermetallics.

The content of this work is organized as follows. In section 2, the structural stability and the preparation procedure of Laves phases are discussed. This is followed by a comparison of the electronic density of states (DOS) properties of Fe, Co and Ni containing compounds. Furthermore, SF and their influence on the physical properties in the RCo_2 compounds is sketched. Section 3 deals with the magnetic stability of the itinerant electron subsystem. Mainly the itinerant electron metamagnetism (IEM) is described. The transport phenomena, primarily of the nonmagnetic RCo_2 compounds, are discussed in section 4. The important role of SF for understanding of the temperature variation of the transport phenomena is shown there. The thermal expansion and magnetostriction of the binary magnetic and nonmagnetic RCo_2 compounds are compared in section 5. The effect of external pressure is considered in section 6. In section 7, examples of binary intermetallics ($TiCo_2$, $ZrCo_2$ and $HfCo_2$) and some pseudobinary systems are presented where the magnetic and transport properties deviate in various aspects from those compounds discussed in the sections before.

2. Crystal structure and electronic properties of the RCo_2 compounds

2.1. Stability of the C15 structure in pseudobinary R(Co,T)$_2$ systems

The RCo_2 compounds crystallize in the $MgCu_2$-type (C15) structure (space group $Fd3m$) (Iandelli and Palenzona 1979), where the R atoms form a diamond lattice and the remaining space inside the cell is occupied by regular tetrahedra consisting of the Co atoms. In this structure, the R and Co atoms each occupy one crystallographic site, namely the 8*a* and 16*b* sites, respectively. The ionic radii ratio among the RCo_2 series (r_R/r_{Co}) varies between 1.26 and 1.24, i.e. it is on average larger than the ideal ratio ($r_R/r_{Co} = 1.225$) for the most dense packed lattice. However in order to show that this ratio is not the only parameter which is responsible for the stability of the C15 type structure we have selected a number of pseudobinary systems and considered the stability of the C15 structure with respect to the partner element. In figure 1 the crystal structures of various $R(Co_{1-x}T_x)_2$ pseudobinary systems are shown as a function of the concentration x. The systems are arranged according to increasing r_T.

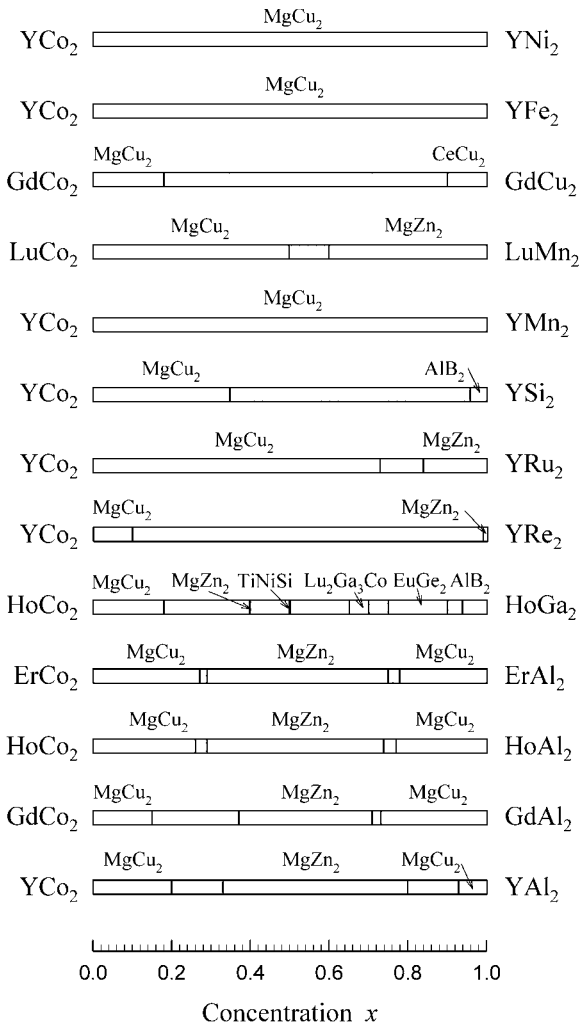

Figure 1. Crystal structures of selected $R(Co_{1-x}T_x)_2$ pseudobinary systems. The hatched areas show the regions where a mixture of two or more phases was obtained.

A solid solubility is known for the systems with Ni, Fe and Mn (3d elements) only, whereas in all the other selected examples at least one concentration region exists with either a different structure type or a multiphase mixture. In some of the selected systems the boundary compounds do not have the C15 structure. $GdCu_2$ crystallizes in the orthorhombic $CeCu_2$-type structure, YSi_2 shows the hexagonal AlB_2-type structure, and YRu_2 and YRe_2 both crystallize in the hexagonal $MgZn_2$-type (C14) structure. Interestingly, although both boundary compounds in the $R(Co_{1-x}Al_x)_2$ systems exhibit the C15 structure, there is an intermediate concentration range where the C14 structure is stable. A complicated situation has been found in the $Ho(Co_{1-x}Ga_x)_2$ system, where several ternary intermetallics have been observed. The conclusion is that the conduction electron concentration, along with the r_R/r_{Co} ratio, determine the crystal structure of the R–3d intermetallics with the 1:2 stoichiometry.

In numerous experimental works it has been reported that for the preparation of a single phase RT_2 sample material with T = Mn, Fe, or Co an excess of the R component is necessary.

The starting composition proposed by different authors varies between 1:1.88 and 1:1.95. At least for RCo_2, this off-stoichiometry cannot be accounted for a preferential evaporation of the R component, because the weight loss observed during the melting procedure normally is within about 0.1%, i.e. it is much less to shift the composition to 1:2. A possible explanation why an off-stoichiometry is necessary might be that the R atoms partly occupy the transition metal sites in the tetrahedra. In the RCo_2 compounds the off-stoichiometry avoids the appearance of the neighbouring RT_3 phase in the phase diagram (that applies especially when non-magnetic RCo_2 intermetallics are investigated, since the respective RCo_3 are ferromagnetic impurities).

An opposite deviation from the 1:2 stoichiometry was found in the RNi_2 series. For the light RNi_2 compounds a single phase sample can be obtained with a nickel excess only, i.e. $R_{1-\delta}Ni_2$, where δ is around 0.05 (depending on the R partner element). This new structure found in the $R_{1-\delta}Ni_2$ series with R = Y, Sm, Gd and Tb is a superstructure of the cubic Laves phase with the space group $F\bar{4}3m$, which is characterized by a doubling of the cubic unit cell parameter and by vacancies on the R sites (Latroche *et al* 1990).

2.2. *Electronic structure of the RCo_2 compounds*

For the YT_2 compounds with T = Fe, Co and Ni several authors have published band structure calculations. Although for these calculations different methods have been used (e.g. Yamada *et al* 1984, Schwarz and Mohn 1984), the common result of all these calculations confirms the existence of a strong hybridization between the 3d states of the transition metal and 4d states of yttrium (or 5d states in the case of a lanthanide). The hybridization is considered as playing an important role for the magnetic properties of these compounds. The calculated energy dependence of the DOS, $N(\varepsilon)$, is qualitatively similar in shape for all these intermetallics. At low energies $N(\varepsilon)$ exhibits a relatively narrow peak (due to the 3d electronic states) followed by a flat range with lower DOS at higher energies (primarily due to the 4d states). In figure 2, $N(\varepsilon)$ near to the Fermi energy, ε_f, of YFe_2, YCo_2 and YNi_2 are compared. The corresponding Fermi levels lie in different regions of the $N(\varepsilon)$ function, which are intimately related to the magnetic properties of these three compounds.

Among them YNi_2 has the lowest value of $N(\varepsilon_f)$. The Stoner criterion of ferromagnetism $IN(\varepsilon_f) \geqslant 1$ (I is the d–d exchange integral) is by far not fulfilled. The product $IN(\varepsilon_f) = 0.21$ (Yamada *et al* 1984), which is much smaller than 1. YNi_2 is nonmagnetic showing a very weak temperature dependence of the susceptibility and the overall value is about the Pauli susceptibility given by $\chi_0(0) = 2\mu_B^2 N(\varepsilon_f)$. In contrast, $N(\varepsilon_f)$ of YFe_2 is much larger, and $IN(\varepsilon_f) = 2.6$. YFe_2 therefore is a strong itinerant ferromagnet ($T_C = 540$ K) and with a spontaneous magnetization $M_S = 1.4\ \mu_B$/Fe at 4.2 K (Fujii *et al* 1983). Since M_S of YFe_2 is considerably smaller than M_S for metallic Fe ($= 2.2\ \mu_B$/Fe), YFe_2 is a non-saturated ferromagnet, i.e. the spin up as well as the spin down band both are not filled. For YCo_2 the Stoner criterion is nearly fulfilled, $IN(\varepsilon_f) = 0.9$. This causes a strong exchange enhancement, with a pronounced temperature variation of the susceptibility. The average value of χ is much larger than the Pauli susceptibility.

The purpose of figure 3 is to explain the magnetization process in the paramagnetic RCo_2 compounds, in a band splitting picture following the arguments given in Yamada (1988). In figure 3 the dashed line denotes ε_f. The rectangles on both sides of the energy axis ε depict schematically the position of the 3d bands (lower) and the 4d (5d) bands. In order to simplify, the 3d states and 4d(5d) states do not overlap in this schematic picture. The symbols $n_{T\uparrow}$, $n_{T\downarrow}$ denote a measure for the 3d states (non-hatched areas) and $n_{R\uparrow}$, $n_{R\downarrow}$ are those for the 4d(5d) states (hatched areas). The hatched areas within the 3d rectangles (in both spin directions) are to show that as a consequence of the hybridization a mixing of the 3d and 4d(5d) electronic

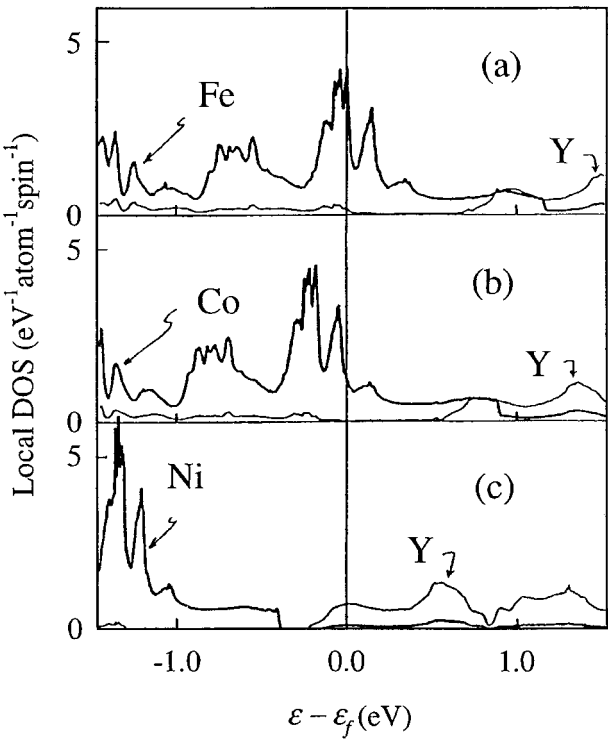

Figure 2. Calculated local DOS of the 3d electrons of T and 4d electrons of Y for YFe_2 (a), YCo_2 (b) and YNi_2 (c) in the paramagnetic state (after Yamada 1988).

states takes place. Accordingly, the non-hatched areas in the upper rectangles mark the 3d states in the 4d(5d) dominated energy range.

In figure 3(a) the paramagnetic state in zero external magnetic field is shown (there is no splitting of any of the bands). Assuming that an external field, B, is applied parallel to the spin up direction, then $n_{T\uparrow}$and $n_{R\uparrow}$ become shifted to lower energies, whereas $n_{T\downarrow}$ and $n_{R\downarrow}$ are shifted to higher energies. Since the interatomic 3d–3d exchange is stronger than the 4d–4d (5d–5d) one, the splitting of the 3d band is larger. In figure 3(b) it can be seen that the distance of the centres of gravity between the 3d and 4d (5d) sub-bands, $\Delta\varepsilon$ (difference between the effective atomic potentials), becomes different for the spin up and spin down directions, i.e. $\Delta\varepsilon\uparrow > \Delta\varepsilon\downarrow$. Since the hybridization decreases with increasing $\Delta\varepsilon$, the number of the 4d(5d) states among the 3d state dominated energy range is then smaller for spin up than for spin down. This can be seen by the difference in the hatched areas ($n_{R\uparrow} < n_{R\downarrow}$) (the actual values for the numbers of electrons labelled by $n_{T\uparrow}, n_{T\downarrow}, n_{R\uparrow}, n_{R\downarrow}$, are obtained by integration of the respective DOS up to ε_f). Consequently the magnetization, M_R ($\propto (n_{R\uparrow} - n_{R\downarrow})$), is negative, i.e. opposite to the external field and to M_T ($\propto (n_{T\uparrow} - n_{T\downarrow})$). In this way the negative orientation of M_R can be understood by the difference of the hybridization between the up and down spin states.

With a magnetic R partner element, the 4f-electron spin moment of the rare earth atom is oriented parallel to its 5d-spin moment, due to the positive intraatomic exchange interaction. Hence, the total R magnetic moment $M_R = g_R\mu_B J_R$ is oriented opposite to the transition metal moment for heavy ($J = L + S$) and parallel to M_T for light ($J = |L - S|$) rare earth elements.

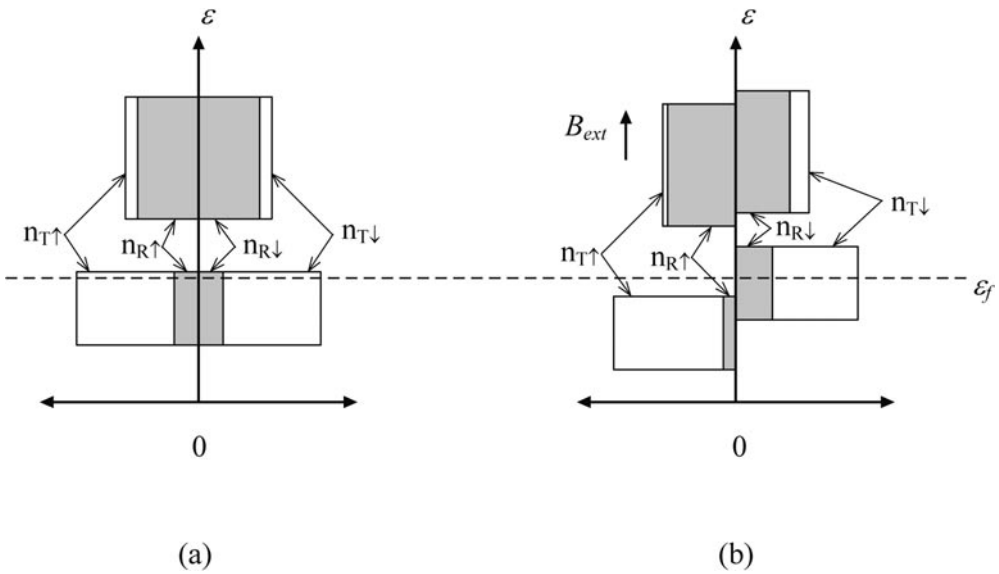

Figure 3. Schematic representation of the local DOS of paramagnetic R–3d intermetallics: (a) in the paramagnetic state, (b) in the magnetized state by an external field (after Yamada 1988). The symbols $n_{T\uparrow}, n_{T\downarrow}, n_{R\uparrow}, n_{R\downarrow}$ denote the measures of the 3d and 4d(5d) states above and below the Fermi level for spin-up (↑) and spin-down (↓) subbands.

2.3. Spin fluctuations in itinerant electron system

In RCo_2 with nonmagnetic R partner elements (Sc, Y or Lu), the ground state is close to the ferromagnetic instability. The corresponding Stoner factors, $S = (1 - IN(\varepsilon_f))^{-1}$ are of the size of 10. This elevated value is mainly due to the high $N(\varepsilon_f)$ in these compounds. Note that a large S-factor can also be due to a large d–d exchange interaction I. On the other hand, an enhanced $N(\varepsilon_f)$ value is a necessary prerequisite for the appearance of SF.

With increasing temperature, thermally induced *fluctuating* magnetic moments have been predicted by the theory (Moriya 1991). Burzo and Lemaire (1992) and Burzo *et al* (1993) have analysed the magnetic susceptibility of the nonmagnetic RCo_2 compounds with R = Sc, Zr, Y, Lu and Hf in a wide temperature range (2 to 900 K) using the SF theory. The χ–T curves for $ScCo_2$, YCo_2 and $LuCo_2$ are presented in figure 4. The temperature variation of $\chi(T)$, which is characterized by a maximum at a certain temperature T_{max}, is qualitatively similar for these intermetallics. The maximum position in $\chi(T)$ was regarded as a cross-over from the low temperature region governed by the temperature variation of SF and the elevated regime when the SF amplitude becomes temperature independent and the material starts to follow a Curie–Weiss behaviour.

From the Curie constants effective Co moments can be estimated, because $N(\varepsilon_f)$ is dominated by the 3d states of Co. The thus obtained μ_{eff} per Co atom for the three RCo_2 compounds are given in figure 4. They are close to the divalent ionic state (Co^{2+}). As can be seen these values depend on whether $ScCo_2$, YCo_2 or $LuCo_2$ is considered. The paramagnetic Curie temperatures estimated from the Curie–Weiss fit are however all negative, which is difficult to understand in the scope of high temperature localization.

On the other hand, starting from DOS calculations and taking additionally into account the effect of SF, Yamada *et al* (1984, 1985) showed that the peak position in $\chi(T)$ can be understood by the properties of the DOS in the vicinity of ε_f.

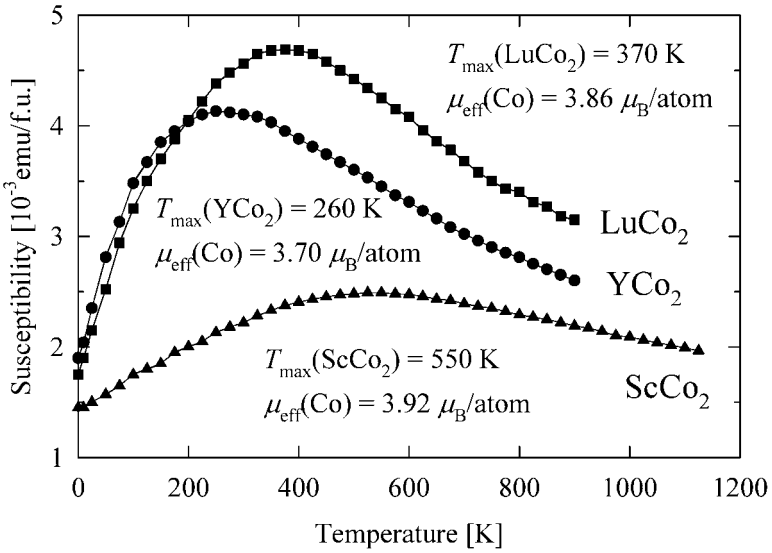

Figure 4. Thermal variation of the magnetic susceptibility in $ScCo_2$, YCo_2 and $LuCo_2$ (Burzo *et al* 1993).

A typical example to show how longitudinal SFs contribute to the magnetic properties can be found in a certain concentration range of the pseudobinary $Y(Co_{1-x}Al_x)_2$ system. The compounds within the region $0.12 \leqslant x_C \leqslant 0.19$ are very weak itinerant ferromagnets (Yoshimura and Nakamura 1985). Two mechanisms have been considered to be responsible for this behaviour: a narrowing of the d band due to the lattice expansion (Sakakibara *et al* 1987) and a shift of the Fermi level towards lower energies with a higher $N(\varepsilon_f)$ value, caused by the decrease of the d-electron concentration (Aleksandryan *et al* 1985).

In the scope of the Landau description of the very weak itinerant ferromagnetism the spontaneous magnetization is given by (Shimizu 1981)

$$M_S(T) \propto \sqrt{1 - (T/T_C)^2}. \tag{1}$$

Taking into account existence of temperature dependent longitudinal SFs, equation (1) is modified (Moriya 1991):

$$M_S(T) \propto \sqrt{1 - (T/T_C)^{4/3}}. \tag{2}$$

The experimental data for the $Y(Co_{1-x}Al_x)_2$ compounds obey the latter relation in expanded temperature regions (Yoshimura and Nakamura 1985).

A detailed quantitative analysis of the magnetic properties of the $Y(Co_{1-x}Al_x)_2$ system within the framework of the self-consistent renormalization theory has been carried out by Yoshimura *et al* (1987) using the magnetization and the ^{59}Co and ^{27}Al spin-echo NMR measurements. The observed temperature dependence of the nuclear spin–lattice relaxation rate $1/T_1$ was found to be described well by the theory in the substituted compounds over a wide temperature range.

3. Magnetic instability of the d-electron subsystem and field induced magnetic phase transitions

3.1. Itinerant electron metamagnetism in external fields

IEM means a field induced first order magnetic phase transition from a paramagnetic into a ferromagnetic state at a critical field, B_M. Also in the case of a ferromagnetic ground state, if there is a field induced increase of $N(\varepsilon_f)$, IEM can occur from a weak ferromagnetic (WFM) to a strong ferromagnetic (SFM) state (Shimizu 1982).

The prerequisite for the appearance of IEM in these compounds is the existence of a local peak in DOS below ε_f and a large positive curvature of $N(\varepsilon)$ in this energy region. Under this condition, the application of an external field causes a substantial increase of $N(\varepsilon_f)$ and the Stoner criterion becomes fulfilled beyond B_M. The phenomenological description of IEM can be given the by Landau expansion of the magnetic free energy up to the sixth power of M

$$F(M) = \tfrac{1}{2}c_1M^2 + \tfrac{1}{4}c_3M^4 + \tfrac{1}{6}c_5M^6 \tag{3}$$

where the coefficients $c_i(T)$ depend on the band characteristics (Shimizu 1982). The necessary condition for the increase of $N(\varepsilon_f)$ under an external field is then the negative sign of the coefficient c_3, and IEM occurs in a paramagnetic compound ($c_1 > 0$ and $c_5 > 0$) when

$$\frac{3}{16} < \frac{c_1c_5}{c_3^2} < \frac{9}{20}. \tag{4}$$

In RCo_2 compounds the estimated B_M field is of the order of 10^2 T (Bloch *et al* 1975). Such fields were far beyond the experimental possibilities in the 1970s. However, it has been observed that B_M decreases in $R(Co_{1-x}T_x)_2$ systems, due to the substitution. This was why the phenomenon of IEM was first experimentally observed in a pseudobinary system, namely in $Y(Co_{1-x}Al_x)_2$ (Aleksandryan *et al* 1985). This system orders ferromagnetically for $x \geqslant 0.12$ (see above). The existence of IEM was also found in the ferromagnetic compounds below T_C: B_M decreases down to 8 T at $x = 0.15$. Nowadays magnetic fields are available in laboratories up to 110 T. This enabled Goto *et al* (1990) to observe IEM in YCo_2 (70 T) and $LuCo_2$ (75 T). As far as the temperature dependence of B_M is concerned, it has been found that in all cases B_M increases with increasing temperature and the anomaly at the magnetization curve gradually vanishes (Goto *et al* 1994a).

A number of studies have been performed in order to understand why a substitution lowers B_M. Three mechanisms were discussed: (i) a shift of ε_f due to the change of the d-electron concentration, n_d (Aleksandryan *et al* 1985), (ii) a change of the d bandwidth due to the variation of the lattice parameter (Sakakibara *et al* 1987) and finally (iii) in the case of a non-transition-metal substitution, the hybridization between the d states and 3p states of T has been considered to be responsible.

Gabelko *et al* (1991) compared the variation of B_M against x in $Y(Co_{1-x}Al_x)_2$, $Lu(Co_{1-x}Al_x)_2$ and in the $(Y_{1-t}Lu_t)(Co_{1-x}Al_x)_2$ system: the third system has been selected to keep the lattice parameter constant due to the simultaneous Al and Lu substitutions. It has been concluded that the change in the interatomic distances has less influence than the change of the d-electron concentration. Murata *et al* (1994) observed a decrease of B_M by studying the $Lu(Co_{1-x}Si_x)_2$ system, in which the change in the lattice parameter is small but n_d varies. Goto *et al* (1994b) studied a system based on $Y(Co_{1-x}T_x)^2$ where n_d is kept constant. For this purpose, the system $Y(Co_{1-x}Ni_{0.5x}Fe_{0.5x})_2$ has been investigated with $x \leqslant 0.03$. It has been reported that B_M does not change significantly when n_d is constant.

The interpretation of all these results was made under the rigid band approximation. However for a higher amount of substitution this approximation is no longer valid. Aoki and

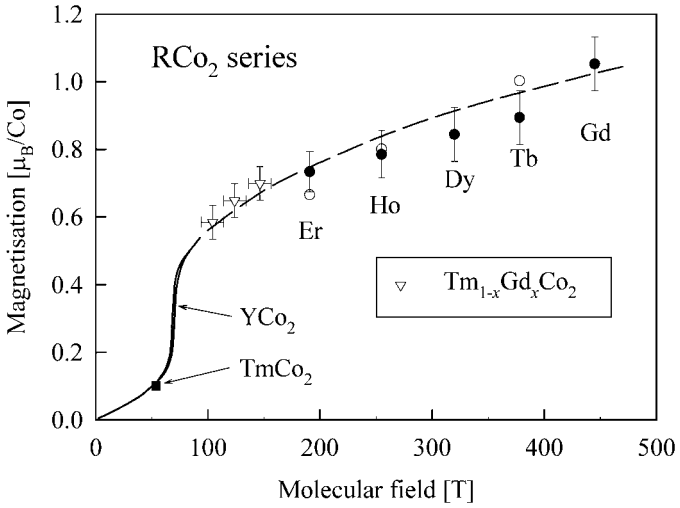

Figure 5. Variation of the d magnetic moment μ_{Co} versus $B_{RCo}^{(Co)}$ derived from the x-ray powder diffraction data of RCo_2 (full circles) and $Tm_{1-x}Gd_xCo_2$ (open down triangles) using equation (20). Open circles represent the single-crystal magnetization data taken from literature (Franse and Radwanski 1993). μ_{Co} for $TmCo_2$ is taken from the neutron diffraction data of Dubenko *et al* (1995). The solid line is the experimental magnetization curve of YCo_2 (Goto *et al* 1990) and the dashed line is drawn as a guide for the eyes.

Yamada (1992) have found that the hybridization between the 3d states of Co and 3p states of the substituent non-transition T atoms becomes important for higher x. The calculations of DOS for $Y(Co_{0.75}Al_{0.25})_2$ revealed that this hybridization causes a substantial change of the shape of $N(\varepsilon)$ around ε_f. The peak in DOS below $N(\varepsilon_f)$, which is responsible for IEM and for the appearance of ferromagnetism in the $R(Co_{1-x}Al_x)_2$ systems, is smeared out.

3.2. Effect of the f–d intersublattice exchange

When R bears a magnetic moment and the R sublattice undergoes a magnetic transition, the itinerant d-electron subsystem (Co sublattice) becomes magnetized. The effective field acting on the Co sublattice can be represented as

$$\boldsymbol{B}_{eff}^{(Co)} = \boldsymbol{B}_{mol}^{(Co)} + \boldsymbol{B}_{ext} = \boldsymbol{B}_{RCo}^{(Co)} + \boldsymbol{B}_{CoCo} + \boldsymbol{B}_{ext} = \lambda_{RCo}\boldsymbol{M}_R = \lambda_{CoCo}\boldsymbol{M}_{Co} + \boldsymbol{B}_{ext} \tag{5}$$

where $B_{RCo}^{(Co)}$ and B_{CoCo} arise from the intersublattice and intrasublattice exchange interactions, respectively, and λ_{RCo} and λ_{CoCo} are the corresponding molecular field coefficients.

Since in RCo_2 $B_{RCo}^{(Co)}$ is much larger than B_{CoCo}, the molecular field acting on the Co sublattice can be set proportional to the magnetization of the R sublattice M_R. The molecular field coefficient λ_{RCo} is expressed through the spin–spin exchange interaction parameter I_{RCo} as $\lambda_{RCo} = I_{RCo}(g_R - 1)/g_R$. Assuming that the dependence of I_{RCo} on the R element is weak, the field acting on the Co sublattice is proportional to $(g_R - 1)S_R$. The metamagnetic behaviour of the Co sublattice within the cobalt Laves phases can clearly be seen when plotting M_{Co} against $B_{mol}^{(Co)}$ (figure 5). The symbols in this plot depict the M_{Co} values as obtained from thermal expansion and magnetization measurements. This figure shows that for all the RCo_2 compounds (except $TmCo_2$) $B_{mol}^{(Co)} > B_M$ thus stabilizing a ferromagnetic order in the Co sublattice. In $TmCo_2$ the Co sublattice remains non-magnetic below T_C (Gratz *et al* 1995a). Brommer *et al* (1993) determined $B_{mol}^{(Co)}$ (= 54 T) for $TmCo_2$, which is below the value of

$B_M = 70$ T necessary to induce ferromagnetic order in the Co sublattice. The magnetization curve of YCo_2 (Goto *et al* 1990) is included in figure 5: it fits well the general tendency of M_{Co} against $B_{mol}^{(Co)}$.

In all RCo_2 compounds M_R is larger than M_{Co}. The external field is therefore parallel to M_R, thus the effective field acting on the Co sublattice decreases (for heavy RCo_2) with increasing external field: $B_{eff}^{(Co)} = B_{mol}^{(Co)} - B_{ext}$. If B_{ext} exceeds a critical field B_{cr}, the Co sublattice magnetization is destabilized and so called 'inverse IEM' may occur. This inverse IEM is visible, e.g., as a steplike increase in the magnetization. Above B_{cr} long range magnetic order exists in the R sublattice, only. This field can be reduced by substitutions. For $R_{1-x}Y_xCo_2$ systems the concentration dependence of B_{cr} is given by

$$B_{cr}(x) \approx (1-x)\lambda_{RCo}M_R - B_M. \tag{6}$$

Among the heavy RCo_2 compounds, $ErCo_2$ has the lowest value of $B_{mol}^{(Co)} = 190$ T (see figure 5) and therefore the lowest expected value of B_{cr}. Indeed, transitions of this type have been observed in the $Er_{1-x}Y_xCo_2$ and $Er_{1-x}Lu_xCo_2$ systems in measurements of the magnetostriction, magnetization and magnetoresistance (Levitin *et al* 1984, Wada *et al* 1994, Hauser *et al* 2001). Selected magnetization curves showing the inverse IEM effect are displayed in figure 6. The transition occurs in $Er_{0.3}Tm_{0.7}Co_2$ (12 T) and $Er_{0.6}Y_{0.4}Co_2$ (8.5 T) in agreement with equation (6).

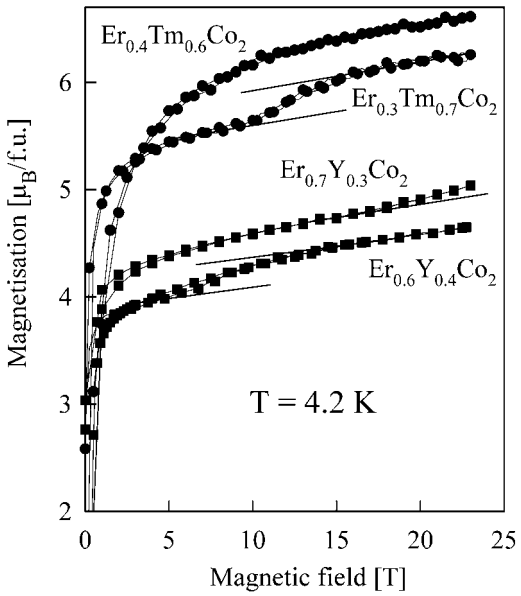

Figure 6. Magnetization curves at 4.2 K of selected $Er_{1-x}R_xCo_2$ (R = Y or Tm) compounds (Hauser *et al* 2001). The solid straight lines are linear extrapolations from the field regions below and above B_{cr}. $Er_{0.3}Tm_{0.7}Co_2$ and $Er_{0.6}Y_{0.4}Co_2$ show inverse IEM at 12 T and 8.5 T, respectively. For $Er_{0.7}Y_{0.3}Co_2$ the critical field exceeds 25 T; however above 20 T an upturn can be seen in the magnetization curve.

Another interesting effect observed in the RCo_2 compounds is that with R = Dy, Ho and Er the magnetic phase transition at T_C is of a first-order type. This phenomenon is however intimately related with the metamagnetic properties of the d subsystem (see Levitin and Markosyan 1988, Duc and Goto 1999). The conditions for the occurrence of a first-order transition at T_C have been given by Bloch *et al* (1975) and Inoue and Shimizu (1988) within

the scope of the molecular field approximation and assuming that the d subsystem is identical throughout the whole RCo_2 series. It was concluded that the magnetic transition is of a first order type when $c_3(T_C) < 0$. Using the equation of state (3) and introducing the magnetic 4f sublattice, the following expressions were derived:

$$T_C^{II} = N\frac{g^2\mu_B^2 J_R(J_R+1)}{3k_B}(\lambda_{RR} + \lambda_{RCo}^2\chi_d(T_C^{II})) \tag{7a}$$

if the magnetic transition is of a second order type, and, when the transition is of a first order type, T_C^I is determined from the equation

$$c_1(T_C^I) = \frac{3}{16}\frac{c_3'^2(T_C^I)}{c_5'(T_C^I)}. \tag{7b}$$

The symbols in equation (7*a*) have their usual meaning, and the coefficients c_i' in equation (7*b*) are those of the Landau expansion modified by the f–d exchange interaction. Within the RCo_2 series the transition is of a first order type when $T_C < 150$ K, for which $c_3'(T_C^I) < 0$.

The first order magnetization process observed in $ErCo_2$, $HoCo_2$ and $DyCo_2$ above T_C is also closely related to the above effect and is a consequence of the positivity of $\partial T_C/\partial B_{ext}$. A jumplike transition from a paramagnetic into a ferrimagnetic state occurs in these compounds at a critical field when T_C is reached (Givord and Shah 1972).

Very recently it has been discovered that a ferrimagnetic system, e.g. RCo_2, can be decoupled if one of the sublattices exhibits a magnetic instability. This phenomenon takes place when (setting $B_{RR}^{(Co)}$ zero)

$$B_{RCo}^{(Co)} < B_{cr} \tag{8a}$$

at $T = T_C^{(R)}$ of the R sublattice, and

$$B_{RCo}^{(Co)} > B_{cr} \tag{8b}$$

holds at 0 K. For these selected compounds the critical condition for the onset of magnetic order in the Co sublattice is not fulfilled at $T_C^{(R)}$; however it will be fulfilled on further cooling thus resulting in a second transition at $T = T_C^{(Co)} < T_C^{(R)}$. A separate ordering of the two magnetic sublattices can be anticipated in substituted $R'_{1-x}R''_xCo_2$ compounds within a limited concentration range (Levitin *et al* 1984).

As an example, figure 7 displays the two separate ordering temperatures ($T_C^{(R)}$ and $T_C^{(Co)}$) in the $Er_{1-x}Y_xCo_2$ system (Hauser *et al* 2000). In the Er rich region one anomaly can be seen, which corresponds to the onset of long range magnetic order in both sublattices. For $Er_{0.6}Y_{0.4}Co_2$, two maxima are observed in the specific heat. From the volume effect accompanying the lower transition it follows that $T_C^{(Co)} = 11$ K, while the R sublattice orders at higher temperature $T_C^{(R)} = 14.5$ K.

3.3. Field induced non-collinear magnetic structures in the presence of a magnetic instability

In ferrimagnets, the antiparallel magnetic configuration can be 'canted' by an external field (Tyablikov 1965). In the range between some critical fields B_{c1} and B_{c2} non-collinear magnetic structures are stable with a linear dependence of M_{tot} against B_{ext}. At $B_{ext} > B_{c2}$ the structure is ferromagnetic.

In case a metamagnetic unstable sublattice exists, the magnetization process in ferrimagnets can be substantially modified (in particular in RCo_2 compounds). If the magnetization of the unstable sublattice (M_{Co}) is less than that of the stable one (M_R) and

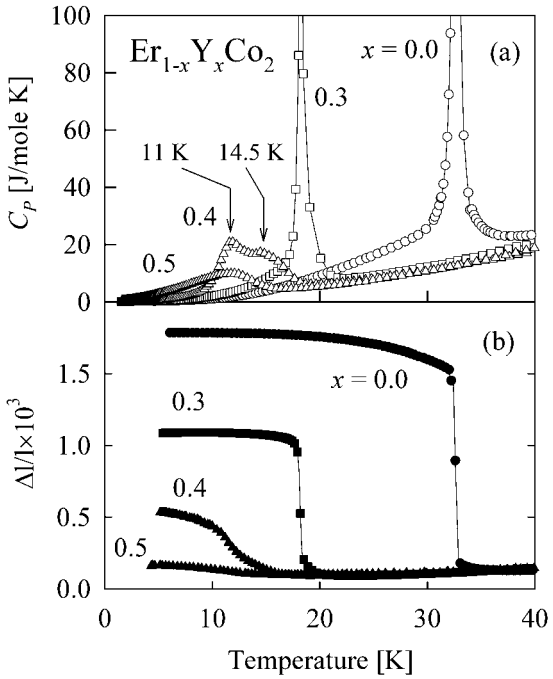

Figure 7. The temperature-dependent specific heat C_P (a) and linear thermal expansion (b) of the $Er_{1-x}Y_xCo_2$ compounds with $x = 0$, 0.3, 0.4 and 0.5 (Hauser *et al* 2000). Arrows indicate the two transitions resolved in $Er_{0.6}Y_{0.4}Co_2$.

simultaneously B_M is less than the lower critical field B_{c1}, non-collinear magnetic structures will not appear. The system will become ferromagnetic through two IEM transitions: (i) a disappearance of the Co magnetic moment at a critical field B_{m1} and (ii) a re-entrant onset of the Co magnetic moment along the field direction at a field $B_{m2} > B_{m1}$ (Dubenko *et al* 1996):

$$\begin{cases} M_{tot} = M_R - M_{Co} & B_{ext} < B_{m1} = \lambda_{RCo}M_R - B_M \\ M_{tot} = M_R & B_{m1} < B_{ext} < B_{m2} = \lambda_{RCo}M_R + B_M \\ M_{tot} = M_R + M_{Co} & B_{ext} > B_{m2}. \end{cases} \tag{9}$$

Depending on the internal parameters, various magnetization processes and even overlapping of IEM and a transition into a non-collinear phase can occur. The internal parameters B_M, λ_{RCo}, M_R or M_{Co} can be changed using appropriate R and Co substitutions. The comparison between B_M and B_{c1} shows that in all the ferrimagnetic RCo_2 compounds the magnetization process must follow the expressions given by equation (9).

Bartashevich *et al* (1998) studied the $(R_{1-t}Y_t)(Co_{1-x}Al_x)_2$ systems in which the Co sublattice is unstable. For $(Ho_{0.8}Y_{0.2})(Co_{0.925}Al_{0.075})_2$ the conditions given by equation (9) are fulfilled and no non-collinear structures were observed in the magnetization process. Instead, pure metamagnetic transitions occur at 13 and 72 T.

Brommer *et al* (1993) studied the $(Tm_{1-t}Lu_t)(Co_{0.88}Al_{0.12})_2$ system with a stable Co sublattice in fields up to 28 T. $Lu(Co_{0.88}Al_{0.12})_2$ has $T_C = 150$ K and $M_S(0) = 1.15\ \mu_B$/fu. In this system, no IEM was found. Instead, non-collinear structures were observed in the concentration region $0.27 \leqslant t \leqslant 0.65$ where B_{c1} is small. From these data $\lambda_{TmCo} = -(13.5 \pm 0.1)$ T/μ_B fu and $\mu_{Tm} = 4.3\ \mu_B$ were evaluated.

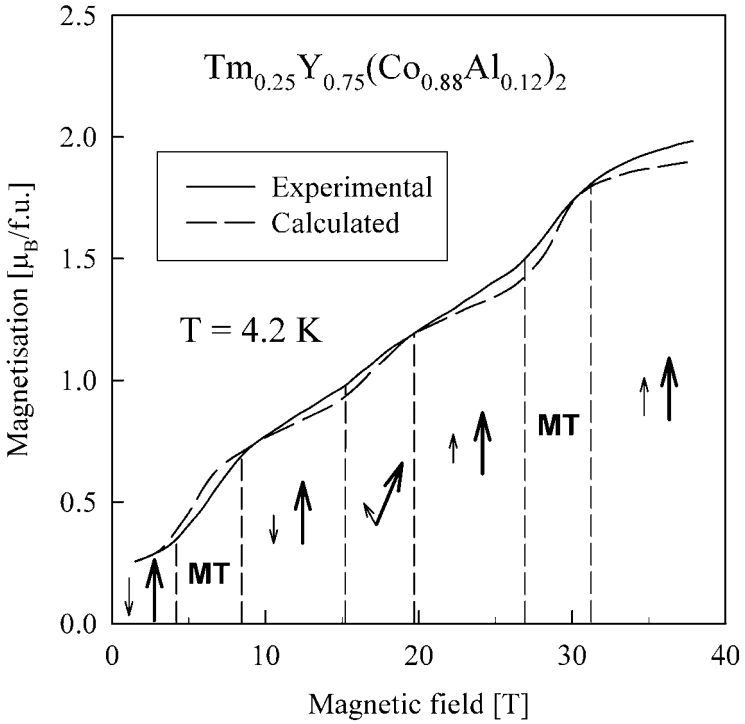

Figure 8. The magnetization curve of $(Tm_{0.25}Y_{0.75})(Co_{0.88}Al_{0.12})_2$ (Brommer *et al* 1995). The vertical dashed lines separate the different magnetic phases, the configuration of which is depicted by thick (R sublattice) and thin (Co sublattice) arrows. MT denotes the field range where IEM occurs.

$Y(Co_{0.88}Al_{0.12})_2$ is a very weak itinerant ferromagnet ($T_C \approx 8$ K, $M_S(0) = 0.08\ \mu_B$/fu) and shows IEM from a WFM to SFM state at 12 T, with the magnetization increasing from $M_{Co}^{(W)} = 0.3\ \mu_B$/fu to $M_{Co}^{(S)} = 0.8\ \mu_B$/fu. $Y(Co_{0.88}Al_{0.12})_2$ was selected to construct ferrimagnets in which transitions of different type can be realized during one magnetization process (Brommer *et al* 1995). The magnetization curve of $(Tm_{0.25}Y_{0.75})(Co_{0.88}Al_{0.12})_2$ shown in figure 8 is characterized by two stepwise transitions and a region of a pronounced curvature between them. The value of M_S is equal 0.24 μ_B/fu. Hence, in zero field $M_{Co} = 0.84\ \mu_B$/fu, i.e. this sublattice is in the SFM state (the molecular field $\lambda_{TmCo}M_{Tm} = 0.25\mu_{Tm}\lambda_{TmCo} = 17.6$ T exceeds B_M). At low external fields, the net magnetization is $M_{Tm} - M_{Co}^{(S)}$. Since $M_{Co}^{(S)}$ is antiparallel to the external field, above the critical value $B_{m1} = \lambda_{TmCo}M_{Tm}(B_{m1}) - B_M = 6.5$ T the net magnetization becomes $M_{Tm} - M_{Co}^{(W)}$ through IEM. Between $B_{c1} = \lambda_{TmCo}(M_{Tm} - M_{Co}^{(W)}) = 15$ T and $B_{c2} = \lambda_{TmCo}(M_{Tm} + M_{Co}^{(W)}) = 19.5$ T a change from the antiparallel into the parallel orientation of M_{Tm} and $M_{Co}^{(W)}$ takes place through a non-collinear phase. Finally, in the parallel phase, the second metamagnetic transition occurs at $B_{m2} = \lambda_{TmCo}M_{Tm}(B_{m2}) + B_M = 29.5$ T and the net magnetization becomes $M_{Tm} + M_{Co}^{(S)}$ (Brommer *et al* 1995).

4. Transport phenomena

It is of general interest to know the behaviour of the transport phenomena as a function of temperature of any material to be studied. This especially holds for YCo_2, since from a

study of the transport phenomena (electrical resistivity, thermal conductivity etc) important information about the nature of SFs and their dynamics can be expected. From these studies also a better understanding of the considerably more complex transport properties of the other RCo_2 intermetallics (where R is magnetic) has been gained (see e.g. Fournier and Gratz 1993).

The transport properties of YCo_2 are summarized below. The data of the other two SF systems ($LuCo_2$ and $ScCo_2$) are included to illustrate the gradual decrease of the SF effect on the transport phenomena from YCo_2 towards $LuCo_2$ and $ScCo_2$.

4.1. Electrical resistivity

Figure 9 shows the temperature dependence of $\rho(T) - \rho_0$ for the three RCo_2 compounds (plus YAl_2 and $LuNi_2$). Both the phonon and the SF scattering cause an increase of $\rho(T)$ with increasing temperature. In order to separate the SF part from the total resistivity one frequently uses Matthiessen's rule:

$$\rho(T) = \rho_0 + \rho_{ph}(T) + \rho_{sf}(T) \tag{10}$$

where the subscripts 0, ph and sf denote the impurity, the phonon and the SF scattering contributions to $\rho(T)$. Under the assumption that $\rho_{ph}(T)$ of the RCo_2 compounds and YAl_2 (or $LuNi_2$) is about the same, one can obtain an estimation of the temperature variation of $\rho_{sf}(T)$. From this analysis a T^2-dependence of $\rho(T) - \rho_0$ in the region up to about 25 to 30 K follows ($\rho_{ph}(T)$ is negligibly small in this region compared to ρ_{sf}). These details are given in the inset of figure 9. The T^2-region is followed by a further increase of ρ_{sf} against T which passes a maximum at about 200–250 K (depending whether YAl_2 or $LuNi_2$ is used to determine $\rho_{ph}(T)$) and decreases monotonically up to 1000 K. The observed low temperature behaviour is in agreement with the theoretically predicted $\rho_{sf} = AT^2$ relation. The pre-factor A is related to the corresponding SF temperature T_{sf} by $A \propto (T_{sf})^{-2}$ (Coqblin *et al* 1978). The thus obtained A-values are $A(YCo_2) = 16$, $A(LuCo_2) = 12$ and $A(ScCo_2) = 4.3$ in units of $n\Omega$ cm K^{-2}. The increasing SF temperature is evidence of a decreasing efficiency of the SF scattering in the temperature variation of the resistivity among these three RCo_2 compounds.

An attempt has been made to rationalize the use of SF spectra, as observed by inelastic neutron scattering, to understand $\rho_{sf}(T)$ of YCo_2 (and $ScCo_2$). The saturation of the resistivity at elevated temperatures may be understood as driven by the hardening of the SF spectrum with increasing temperature (Gratz *et al* 2000).

4.2. Thermal conductivity

The temperature variation of the thermal conductivity for the three SF compounds is given up to room temperature in figure 10. The $\lambda(T)$ curve for YAl_2 is also depicted in this figure. For the RCo_2 compounds a strong negative curvature of $\lambda(T)$ in the region 20 K $\leqslant T \leqslant$ 60 K characterizes these curves. For temperatures higher than about 50 K, $\lambda(T)$ is nearly constant and decreases with respect to its magnitude from $ScCo_2$ towards YCo_2. There is a curvature in $\lambda(T)$ of YAl_2; however it is much less pronounced because of the missing SF scattering.

The total thermal conductivity can be written as (Gratz *et al* 1995b)

$$\lambda(T) = (\lambda_e + \lambda_l) = (W_{e,0} + W_{e,ph} + W_{e,sf})^{-1} + \lambda_l \tag{11}$$

(where λ_e and λ_l denote the electronic and the lattice thermal conductivity). For the subdivision of the electronic thermal resistivity ($W_e = 1/\lambda_e$) Matthiessen's rule has again been used. Taking into consideration the calculated temperature dependences for the different scattering

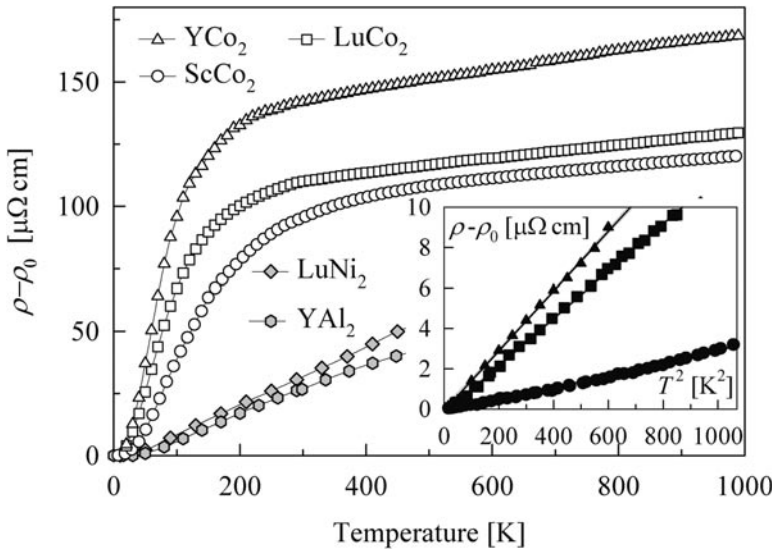

Figure 9. The electrical resistivity ($\rho-\rho_0$) of $ScCo_2$, YCo_2 and $LuCo_2$ ($\rho_0 = 18, 24$ and 17 $\mu\Omega$ cm, respectively) (Gratz 1997). The $\rho(T)$ increase in non-SF systems YAl_2 and $LuNi_2$ ($\rho_0 = 5.6$ and 4.2 $\mu\Omega$ cm) is shown for comparison. Inset: low temperature T^2 dependence of the SF systems.

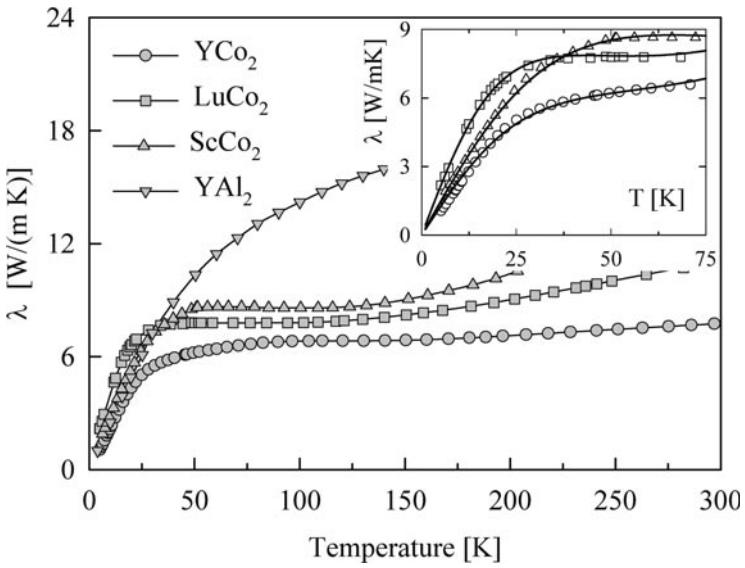

Figure 10. The thermal conductivity of $ScCo_2$, YCo_2, $LuCo_2$ and YAl_2 (Gratz 1997). Inset: fit of equation (12) to the experimental data (given by the lines through the symbols).

contributions: $W_{e,0} = aT^{-1}$, $W_{e,ph} = bT^2$, $W_{e,sf} = cT$ and $\lambda_l = dT^2$, equation (11) is now given by

$$\lambda(T) = (aT^{-1} + bT^2 + cT)^{-1} + dT^2. \tag{12}$$

A least squares fit of this expression to the experimental data up to 75 K is represented by the solid lines in the inset of figure 10. From the comparison of the fit parameters b

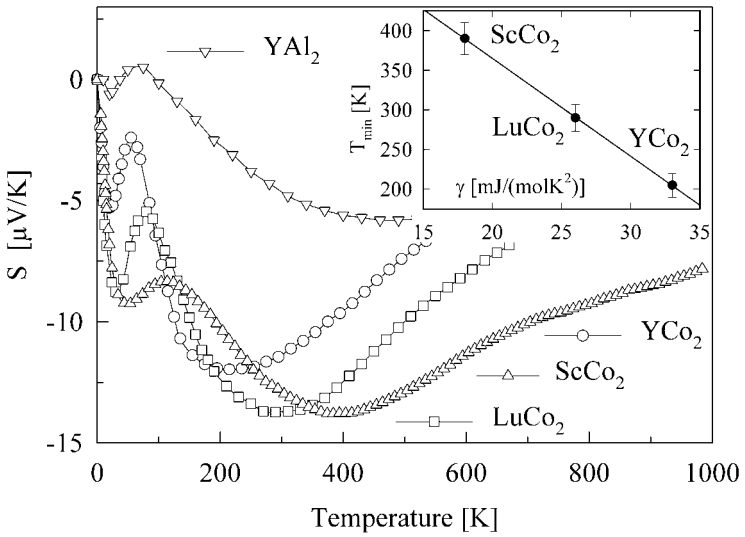

Figure 11. The thermopower of $ScCo_2$, YCo_2, $LuCo_2$ and YAl_2 (Gratz 1997). Inset: correlation between the position of the high-temperature minima T_{min} and value of the specific heat in $ScCo_2$, YCo_2 and $LuCo_2$.

and c it follows that in the SF systems the electron–phonon term $W_{e,ph}$ is much smaller compared to $W_{e,sf}$. The SF term $W_{e,sf}$ dominates the low temperature behaviour of $\lambda(T)$: it is responsible for the typical 'SF induced' curvature between 20 K and 60 K. This is quite in contrast to the case of YAl_2 where the moderate curvature up to about 150 K is due to the phonon scattering part. The c-values (in $W_{e,sf}$) which are related to the SF temperature by $c \propto (T_{sf})^{-1}$ (Coqblin *et al* 1978) are $c(YCo_2) = 23 \times 10^{-5}$, $c(LuCo_2) = 21 \times 10^{-5}$ and $c(ScCo_2) = 11 \times 10^{-5}$ in units of cm mW^{-1}. From the falling tendency of the c-values and the coefficients A in $\rho_{sf}(T)$ it follows that $T_{sf}(YCo_2) < T_{sf}(LuCo_2) < T_{sf}(ScCo_2)$.

4.3. Thermopower

Figure 11 shows the temperature variation of the thermopower of the nonmagnetic RCo_2 compounds (YAl_2 is again included). These $S(T)$ curves (also those for YAl_2) are characterized by two minima, one at low and the other at elevated temperatures. The shallow minimum in $S(T)$ of YAl_2 has been referred to the 'phonon drag' effect (Gratz and Nowotny 1985). Such a 'drag effect' is thought to be caused by the circumstance that beside the conduction electron system other subsystems (phonons or magnons) are thermally in non-equilibrium as well and may cause an additional contribution to the total thermopower, S_{tot}. This is usually taken into account by $S_{tot} = S_{diff} + S_{drag}$, where S_{diff} and S_{drag} are the diffusion and the drag terms, respectively (Ziman 1960). The much more pronounced minima in the SF systems are attributed to a 'paramagnon drag' effect (Gratz 1997). The broader minima at much higher temperatures (below and above the room temperature) are intimately correlated with properties of DOS at ε_f, when the temperature changes (Gratz *et al* 1995b). This has been concluded from the correlation between the position of the high temperature minima T_{min} and the γ-value of the electronic specific heat in $ScCo_2$, YCo_2 and $LuCo_2$ (see the inset in figure 11).

4.4. Magnetoresistance

The temperature and field dependence of the magnetoresistance of YCo_2 is given in figure 12. In order to see the influence of the SF scattering on the magnetoresistance we again inspect the behaviour of the non-SF compound YAl_2, whose data are given in figure 13. These data represent the *transversal* magnetoresistance defined by

$$\frac{\Delta\rho_\perp}{\rho} = \frac{\rho(B,T) - \rho(0,T)}{\rho(0,T)}. \tag{13}$$

The field effect on ρ described by equation (13) is considered as consisting of two parts, one originates from the influence of the magnetic field on the conduction electron trajectories. In between the collision events, the Lorentz force deflects the electrons on their way through the specimen. This mechanism always increases the resistivity in an external field, i.e. it gives rise to positive $\Delta\rho/\rho$-values. This is called *normal magnetoresistance*.

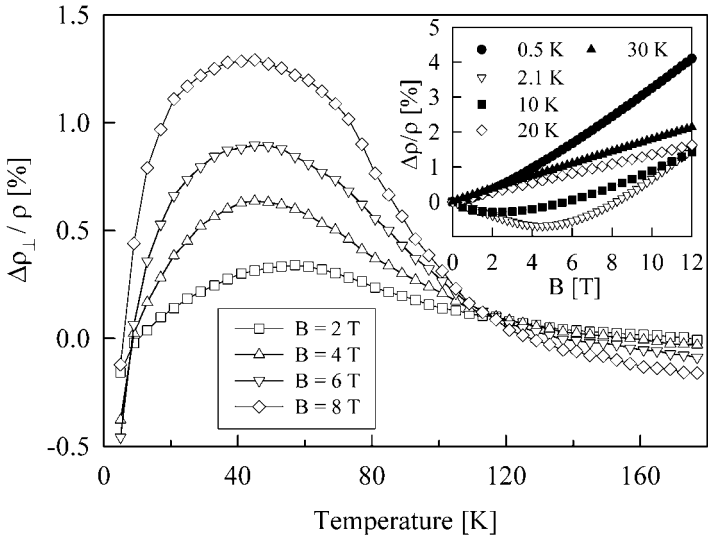

Figure 12. The temperature variation of the magnetoresistance of YCo_2 for various external fields (Gratz 1997). Inset: the field dependence for low temperatures.

In practice, one distinguishes between two limiting cases known as the 'low' and the 'high' field limits. Usual experimental conditions with a polycrystalline sample material lie always in the low field limit, where the conduction electrons traverse a path in a plane perpendicular to the field and complete only a small arc before being scattered. It is assumed that the normal magnetoresistance is the only mechanism which determines the temperature variation of $\Delta\rho/\rho$ in YAl_2. The increase of the $\Delta\rho/\rho$–T curves (shown in figure 13) towards low temperatures in a finite field is thus due to the decreasing electron–phonon scattering. This normal magnetoresistance can be approximated by the following formula (see Gratz 2001):

$$\frac{\Delta\rho_\perp}{\rho} = \frac{B^2}{a[\rho(0,T)] + bB^2} \tag{14}$$

where a and b are field and temperature independent parameters depending on conduction electron properties (band structure), and $\rho(0,T)$ is the total resistivity in zero field. In non-SF compounds, $\rho(0,T)$ is analytically given by the Bloch–Grüneisen relation (ρ_{ph}) plus the residual resistivity (ρ_0). It should be pointed out that in order to obtain a non-vanishing

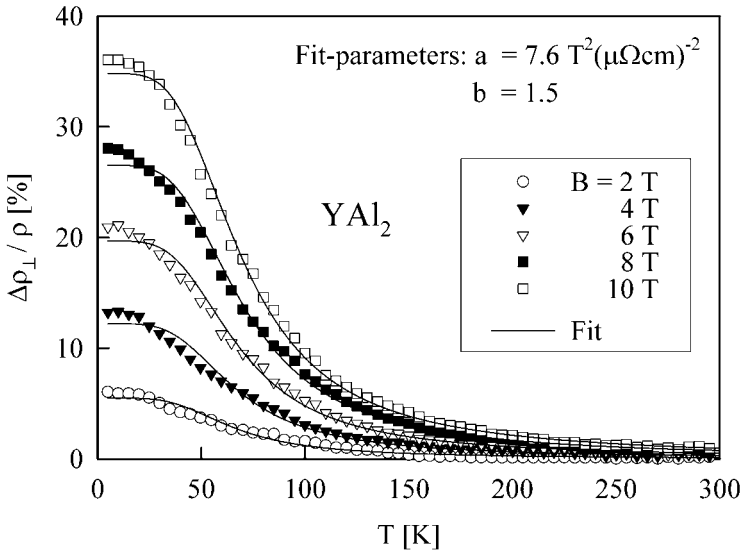

Figure 13. The temperature variation of the magnetoresistance of the non-SF system YAl_2 for various external fields.

magnetoresistance it is necessary to assume that there are two different conduction bands involved in the conduction mechanism (e.g. s and p bands). The solid lines in figure 13 are the results of a least squares fit of equation (14) to the YAl_2 magnetoresistance data.

If there are atoms bearing magnetic moments in the crystal, the external field lines up the moments (in the paramagnetic or ferromagnetic state) and reduces the thermally induced disorder among the magnetic moments. Thus a magnetic field causes a negative magnetoresistance. Such an effect is assumed to exist in SF systems (like in YCo_2) as well. The observed decrease of $\Delta\rho_\perp/\rho$ for YCo_2 towards the lowest temperatures is the consequence of the competition of the normal magnetoresistance (which dominates at higher temperatures) and the growing negative magnetoresistance due to the suppression of SF. The inset in figure 12 displays this tendency for YCo_2 for selected temperatures. The maximum in $\Delta\rho_\perp/\rho$ against T is the result of the suppression of thermal induced SF. The $\Delta\rho_\perp/\rho$–T behaviour for $LuCo_2$ and $ScCo_2$ is qualitatively the same and thus supports the above conclusion.

5. Thermal expansion and magnetostriction

5.1. Thermal expansion and magnetostriction of YCo_2

In order to study the influence of SF on the thermal expansion the data of YCo_2 and data of isostructural non-SF systems, YAl_2 and YNi_2, were compared (Gratz and Lindbaum 1994). In figure 14 the linear thermal expansion of these compounds

$$\frac{\Delta l}{l} = \frac{l(T) - l(T_0)}{l(T_0)} \approx \frac{1}{3}\frac{V(T) - V(T_0)}{V(T_0)} = \frac{1}{3}\omega \tag{15}$$

as obtained from temperature dependent x-ray diffraction is shown (T_0 is the reference temperature to which the data are normalized).

Assuming that the total linear thermal expansion is the sum of an electronic $(\Delta l/l)_{el}$, a phononic $(\Delta l/l)_{ph}$ and a magnetoelastic $(\Delta l/l)_{mag}$ part, it can be written as

$$(\Delta l(T)/l)_{tot} = (\Delta l(T)/l)_{el} + (\Delta l(T)/l)_{ph} + (\Delta l(T)/l)_{mag}. \tag{16}$$

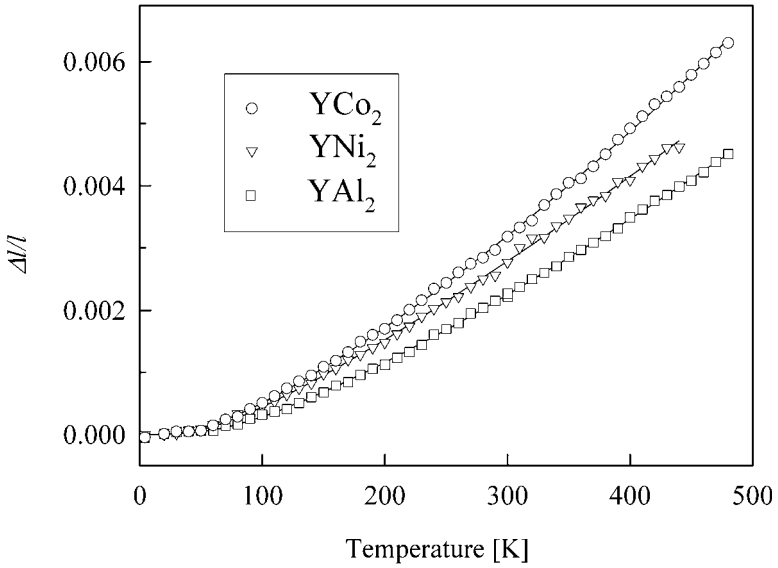

Figure 14. The linear thermal expansion of YAl_2, YNi_2 and YCo_2 (Gratz and Lindbaum 1994).

The temperature variation of these contributions can be approximated by the following analytical relations (Barron *et al* 1980):

$$(\Delta l(T)/l)_{el} = K_1 T^2 \tag{17a}$$

$$(\Delta l(T)/l)_{ph} = K_2 T D(\Theta_D/T) \qquad \text{with } D(z) = (3/z^3)\int_0^z \frac{x^3\,\mathrm{d}x}{\mathrm{e}^x - 1} \tag{17b}$$

where Θ_D is the Debye temperature. A temperature dependence for $(\Delta l(T)/l)_{mag}$ in the presence of SF, at least for the low temperature limit, was given by Yamada (1993):

$$(\Delta l(T)/l)_{mag} \equiv (\Delta l(T)/l)_{sf} = K_1' T^2. \tag{18}$$

From equations (16)–(18) we obtain

$$(\Delta l(T)/l)_{tot} = (K_1 + K_1')T^2 + K_2 T D(\Theta_D/T). \tag{19}$$

The solid lines in figure 14 show the result of the fit procedures of equation (19) to the experimental data. Table 1 gives the obtained fit parameters.

Table 1. Coefficients K_1, K_1' and K_2 and the Debye temperature of YCo_2, YNi_2 and YAl_2 evaluated by fitting equation (19) to the experimental data.

Compound	$K_1 + K_1'$ [K^{-2}]	K_2 [K^{-1}]	Θ_D [K]
YCo_2	$(9.2 \pm 0.6) \times 10^{-9}$	$(1.06 \pm 0.04) \times 10^{-5}$	(226 ± 11)
YNi_2	$(4.0 \pm 1.0) \times 10^{-9}$	$(1.11 \pm 0.06) \times 10^{-5}$	(245 ± 15)
YAl_2	$(4.5 \pm 0.5) \times 10^{-9}$	$(0.94 \pm 0.04) \times 10^{-5}$	(322 ± 10)

The conclusions which have been drawn from a comparison of these parameters are the following.

(i) The much larger parameter $(K_1 + K_1')$ evaluated for YCo_2 can be referred to a finite K_1' caused by the enhanced SF contribution to the thermal expansion.

(ii) The theoretically predicted SF contribution to the thermal expansion is valid (within the resolution of these data) not only at low temperatures.

The volume magnetostriction, ω_B, is related to the magnetization by

$$\omega_B = \frac{V(B,T) - V(0,T)}{V(0,T)} = kCM^2 \tag{20}$$

where k is the isothermal compressibility and C the magnetoelastic coupling constant. For a paramagnet (YCo_2) it follows

$$\omega_B = kC(\chi B)^2. \tag{21}$$

In figure 15 the magnetostriction of YCo_2 at 80 K in fields up to 32 T is shown. Since the susceptibility of YCo_2 is known, equation (21) allows us to determine the *coefficient of the magnetovolume coupling kC*. Its value is $12 \times 10^{-3}\ \mu_B^{-2}$/Co (Markosyan and Snegirev 1985). Figure 15 also includes the *anisotropic* magnetostriction, which is defined as $\lambda_a = \lambda_\parallel - \lambda_\perp$, where $\lambda_\parallel$ and $\lambda_\perp$ are the normalized length changes of the sample, measured in a magnetic field which is either parallel or perpendicular to the expansion measurements, respectively. The value of λ_a reaches -0.5×10^{-5} in a field of 30 T.

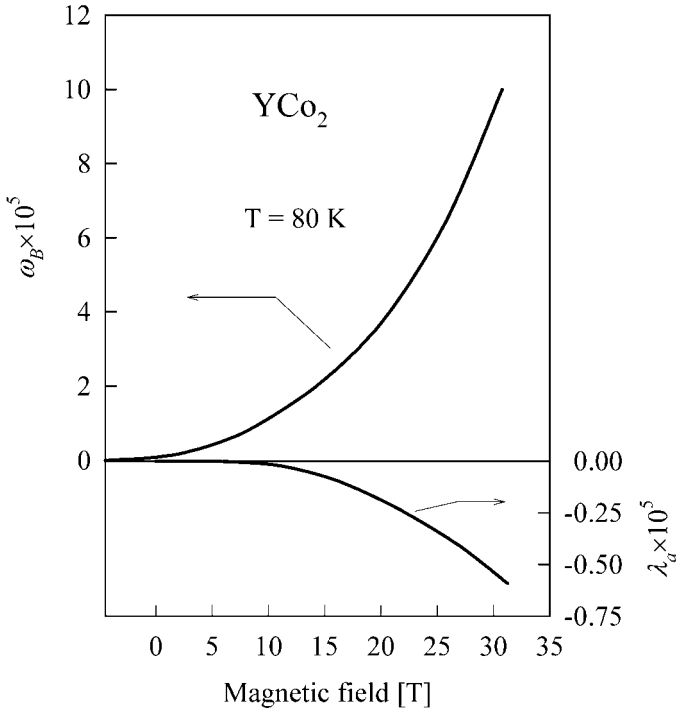

Figure 15. Magnetostriction of YCo_2 measured in pulsed magnetic fields at 80 K (Markosyan and Snegirev 1985).

Goto and Bartashevich (1999) have investigated the forced volume magnetostriction for various concentrations of $Y(Co_{1-x}Al_x)_2$ and $Lu(Co_{1-x}Ga_x)_2$ samples at low temperatures, where the thermal induced SFs are absent. They observed a decrease of the coefficient kC with substitutions (from $15 \times 10^{-3}\ \mu_B^{-2}$/Co for $x = 0.0$ to $10 \times 10^{-3}\ \mu_B^{-2}$/Co for $x = 0.1$). These results were analysed taking into account the contribution from quantum zero-point SFs. A modified coefficient kC was introduced in the form $kC = (kC)_0 - \overline{kC}$ where the

second term is referred to zero-point SFs. The concentration dependence of kC was attributed to changes of the SF spectrum.

5.2. Thermal expansion and magnetostriction in magnetic RCo_2 compounds

The thermal expansion measurements of magnetic RCo_2 show significant anomalies at their Curie temperatures. In figure 16, $(\Delta l/l)$–T curves of some selected RCo_2 compounds are depicted. These data are normalized to the corresponding room temperature values (the arrows indicate T_C). This figure also includes $(\Delta l/l)$ against T of YCo_2. As can be seen, $(\Delta l/l)$ against T in the paramagnetic state is similar (within the resolution of the x-ray diffraction data) for all these compounds. From the measured spontaneous magnetovolume effect of the magnetic RCo_2 compounds the spontaneous Co moments M_{Co} can be calculated using equation (20); this has been done by several authors (see section 3 and Duc and Goto 1999). The M_{Co} values thus obtained are in good agreement with those values determined from the magnetization measurements. The inset in figure 16 shows the corresponding data for $TmCo_2$, which represents an exception with an opposite (negative) change of $(\Delta l/l)$ against T at T_C. This is because the exchange field in this compound is not sufficient to produce moments on the Co sites.

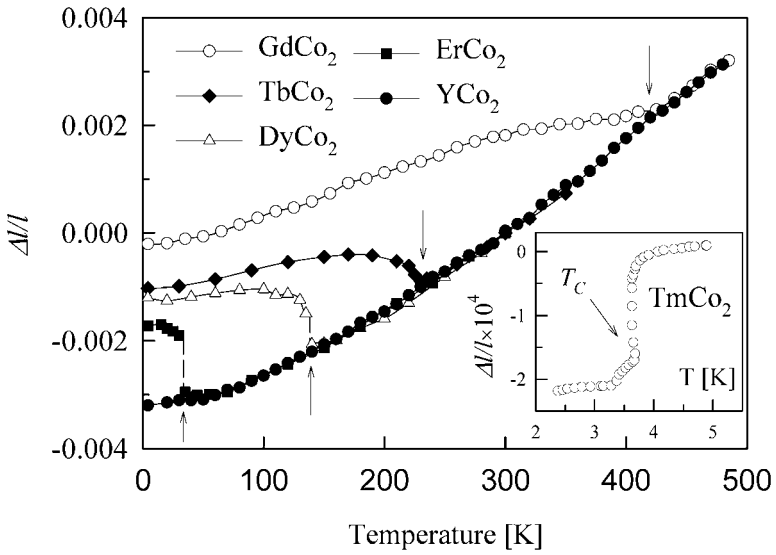

Figure 16. The linear thermal expansion of some RCo_2 compounds normalized to 300 K (Gratz and Lindbaum 1994). The arrows indicate the magnetic ordering temperatures. Inset: the low-temperature behaviour of $\Delta l/l$ for $TmCo_2$.

Below T_C the cubic unit cell of RCo_2 is distorted due to the *spontaneous anisotropic magnetostriction* (see, e.g., Gratz *et al* 1994). In order to describe the anisotropic magnetostriction in cubic crystals, two magnetostriction constant λ_{111} and λ_{100} are used, which characterize the distortion along the two high symmetry directions $\langle 111 \rangle$ and $\langle 100 \rangle$, respectively. The analytic expression is given by

$$\lambda_{anis} = \frac{3}{2}\lambda_{100} \sum_i \alpha_i^2 \beta_i^2 + 3\lambda_{111} \sum_{i<j} \alpha_i \alpha_j \beta_i \beta_j \tag{22}$$

where $i, j = x, y, z$. Here α_i and β_i are the direction cosines between the easy direction of

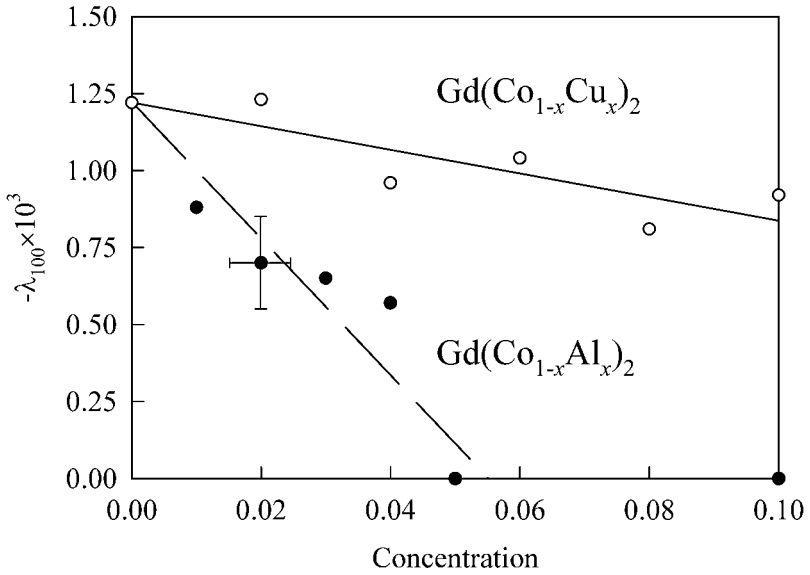

Figure 17. The temperature dependence of the anisotropic magnetostriction constant λ_{100} of the $Gd(Co_{1-x}T_x)_2$ systems with T = Al and Cu at 5 K.

magnetization (easy axis) and the direction of the deformation in the unit cell. The temperature dependent x-ray diffraction technique is an appropriate method to measure λ_{anis} especially if no single crystals are available.

Aleksandryan *et al* (1987) applied an extrapolation method to $(R'_{1-x}R''_x)Co_2$ systems, where the boundary compounds ($R'Co_2$ and $R''Co_2$) have different easy axes, in order to determine the magnetostriction constants λ_{111} and λ_{100} for the RCo_2 compounds. These experiments showed that λ_{111} as a function of RE follows well the theoretical prediction based on the single-ion model (Tsuya *et al* 1964)

$$\lambda_i \propto \alpha_J J_R (J_R - 1) \langle r_{4f}^2 \rangle \tag{23}$$

where λ_i is either λ_{111} or λ_{100}, α_J is the second order Stevens coefficient and $\langle r_{4f}^2 \rangle$ is the mean squared radius of the 4f shell. It was, however, found that λ_{100} does not obey equation (23). λ_{100} is negative in all RCo_2 compounds except $TmCo_2$. Measurements performed on $GdCo_2$ have given a value of -1.2×10^{-3} for λ_{100}, which is comparable with those evaluated for the compounds with $L_R \neq 0$ (Levitin *et al* 1982). It was therefore concluded that the Co sublattice contributes to the anisotropic magnetostriction, due to existence of an orbital part in total M_{Co}.

The origin of this contribution is not yet properly understood. As shown in figure 17, the Co anisotropic magnetostriction is very sensitive to substitutions. In $Gd(Co_{1-x}Al_x)_2$ the value of λ_{100} decreases by more than one order of magnitude for $x \approx 0.05$, while in $Gd(Co_{1-x}Cu_x)_2$ the decrease of λ_{100} for the same x is only about 10%. The variation of λ_{100} against x in the $Gd(Co_{1-x}Al_x)_2$ system is inconsistent with the single-ion model, since the Al substitution should favour an increasing localization of the 3d-electron states at the Co sites due to the increasing Co–Co distance (note $r_{Al} > r_{Co}$). On the other hand, the 3d orbital part seems to remain stable up to at least $x = 0.10$ in $Gd(Co_{1-x}Cu_x)_2$.

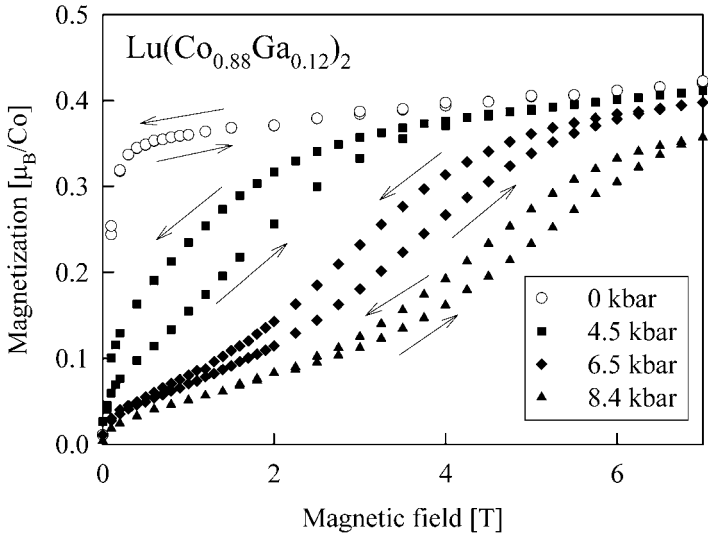

Figure 18. The magnetization curves of $Lu(Co_{0.88}Ga_{0.12})_2$ at 4.2 K for different external pressures (Goto *et al* 1994a).

6. Influence of pressure on the physical properties of RCo_2

The pressure effect can generally be expressed in a variation of the interatomic distances, which changes the magnitude of the exchange integrals and particularly in itinerant electron systems broadens the d band. The latter mechanism is dominant in magnetic itinerant systems; it is responsible for the large negative values of dT_C/dP and the stability of d magnetism in RCo_2, due to a d-band broadening, accompanied in general by a decrease of $N(\varepsilon_f)$.

For paramagnetic IEM it was found that $\chi(T_{max})$ decreases, while T_{max} is pressure independent (T_{max} is the temperature where $\chi(T)$ shows its maximal value) (Yamada 1993). It has been shown that $\partial B_M/\partial P$ is positive and the metamagnetic transition disappears above a certain pressure P_0. The value of P_0 depends on the d-band DOS and the mean square amplitude of the fluctuating magnetization in the paramagnetic state, as well as on the magnetoelastic coupling. P_0 decreases continuously with increasing temperature towards zero at a characteristic temperature T_0.

6.1. Pressure studies of $Lu(Co_{1-x}Ga_x)_2$ intermetallics

Goto *et al* (1994a) measured the magnetization of the ferromagnetic $Lu(Co_{0.88}Ga_{0.12})_2$ under pressure (figure 18). With increasing pressure, a metamagnetic transition appears and $B_M(P)$ increases linearly with a rate of $\partial B_M/\partial P \approx 1.0$ T kbar^{-1}. The authors considered the hybridization between the Co d and Ga p states as being responsible for the stabilization of the ferromagnetic ground state in the $Lu(Co_{1-x}Ga_x)_2$ system. The application of pressure broadens the d band and thus increases the distance between the Fermi level and the high energy peak position in the DOS. The susceptibility of these compounds decreases under pressure in accordance with the prediction of Yamada's calculations. The maximum in $\chi(T)$ at T_{max} shifts however towards lower temperatures. This was referred to the suppression of SF by the external pressure (Yamada 1993).

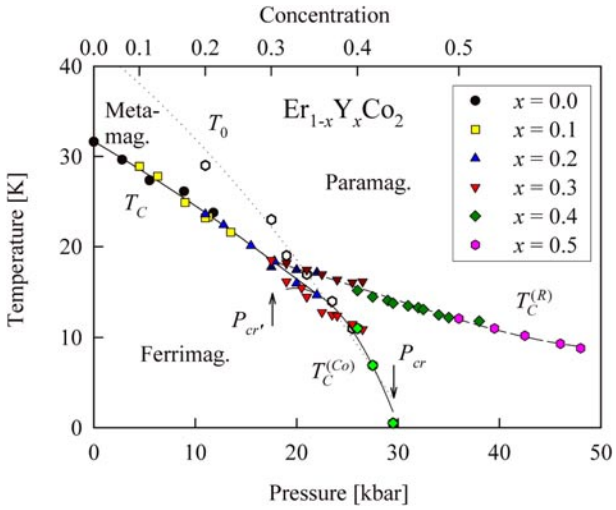

Figure 19. The magnetic phase diagram of the $Er_{1-x}Y_xCo_2$ system as a function of x and external pressure (Hauser *et al* 2000). Solid and dashed lines represent the first- and second order phase boundaries; T_0 limits the temperature up to which IEM is possible.

6.2. Magnetic RCo_2 compounds

For magnetic RCo_2 with $B_{RCo}^{(Co)} > B_M$ the influence of pressure on T_C was calculated by Inoue and Shimizu (1988) using equations (7*a*) and (7*b*). The pressure effect was then analysed assuming that only the Co sublattice susceptibility, $\chi_d(T)$, depends on the volume, thus neglecting the volume dependence of the molecular field coefficients λ_{RR} and λ_{RCo}. Using this approximation Inoue and Shimizu (1988) have calculated the boundary between first and second order magnetic transitions in the RCo_2 compounds as a function of volume change. Their results are in satisfactory agreement with the experimental data of Voiron and Bloch (1971).

Hauser *et al* (2000) observed a pressure induced separation of the ordering temperatures for the R ($T_C^{(R)}$) and Co ($T_C^{(Co)}$) sublattices in $Er_{1-x}Y_xCo_2$, which originates from the metamagnetism of the Co sublattice and different pressure dependence of $T_C^{(R)}$ and $T_C^{(Co)}$. It was found that $\partial T_C^{(Co)}/\partial P > \partial T_C^{(R)}/\partial P$. It has been shown that the application of pressure is comparable with a substitution of Y for Er. In figure 19 the $T_C(P)$ and $T_C(x)$ phase diagrams of the $Er_{1-x}Y_xCo_2$ system are combined. Here the various pressure-dependent characteristic temperatures of the substituted compounds obtained from the $M(B)$ and $\rho(T)$ measurements are positioned in such a way that they match each other, thus resulting in a unified magnetic phase diagram. As can be seen, there is only one Curie temperature up to about $x = 0.3$ or a pressure of roughly 18 kbar. For higher x values and pressures two separate ordering temperatures have been observed. Note that $T_C^{(Co)}$ decreases much faster with increasing x or pressure. For $x > 0.43$ or $P > 30$ kbar no long range magnetic order exists in the Co sublattice; only the R sublattice forms a ferromagnetic state below the corresponding temperature $T_C^{(R)}$. The solid and dashed lines in figure 19 represent the first and second order phase boundaries, respectively. P_{cr} and P'_{cr} mark the respective critical pressures. The dotted line limits the temperature range up to which IEM is possible (T_0). This gives the pressure variation of B_M, the critical field of IEM for the d subsystem, proportional to $P^{4/3}$.

7. Borderline cases

7.1. Lutetium based intermetallics

Although YCo_2 and $LuCo_2$ show almost identical magnetic and transport properties, a substitution of Co by Al has a remarkably different result in $Y(Co_{1-x}Al_x)_2$ and $Lu(Co_{1-x}Al_x)_2$. In the Lu based system a narrow concentration range ($0.1 < x < 0.14$) has been observed where T_C are substantially higher than in $Y(Co_{1-x}Al_x)_2$, even higher than those measured in the $Tm(Co_{1-x}Al_x)_2$ system in the corresponding concentration range. The Curie temperatures of the $Lu(Co_{1-x}Al_x)_2$ system within this concentration range are of the same order of magnitude as those measured in the $Er(Co_{1-x}Al_x)_2$ and $Ho(Co_{1-x}Al_x)_2$ systems (Aleksandryan *et al* 1984).

Dubenko *et al* (1992) studied the substitution of Tm by Lu in $(Lu_{1-t}Tm_t)(Co_{0.88}Al_{0.12})_2$. It was found that T_C increases from 80 K up to 150 K when replacing magnetic Tm by nonmagnetic Lu. In order to clarify the reason for the differences between the Y and the Lu based pseudobinary compounds, Dubenko *et al* (1994a) studied the $(Y_{1-t}Lu_t)(Co_{0.88}Al_{0.12})_2$ system. Figure 20 shows the concentration dependence of M_S and B_M at 4.2 K. It has been found that there exists a critical Lu concentration $t_c \approx 0.4$ above which the 'Y-like' behaviour vanishes and a 'Lu-like' behaviour appears. For $t < t_c$ a WFM state with $M_S = 0.1\ \mu_B$/fu (nearly independent of t) is the stable ground state. In this WFM state metamagnetic transitions are observed. The decrease of B_M with increasing t is given in figure 20 by the square symbols. For higher Lu concentrations an SFM state exists in this system where M_S exceeds $0.9\ \mu_B$/fu, with a slightly increasing tendency towards $t = 1$. There is a sharp transition from the 'Y-like' into the 'Lu-like' ground state; however no metamagnetic transitions are observed in the 'Lu-like' state.

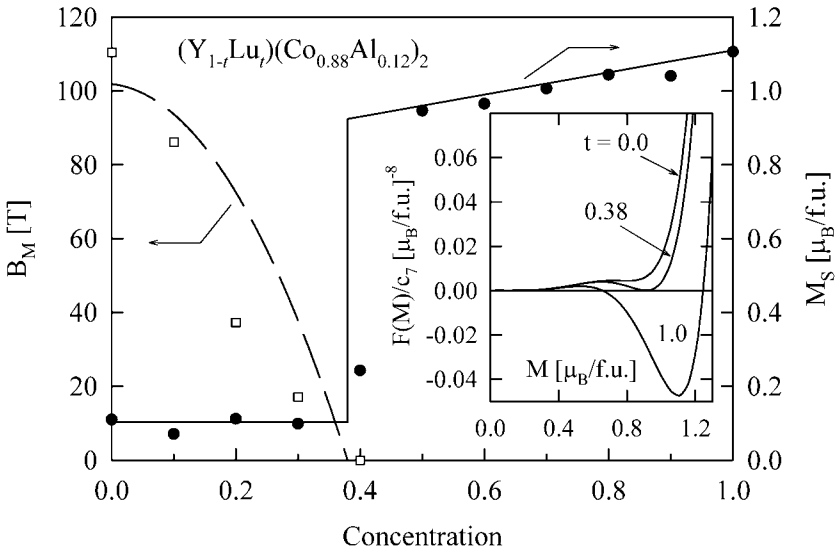

Figure 20. The concentration dependence of M_S (full symbols) and B_M (open symbols) of the $(Y_{1-t}Lu_t)(Co_{0.88}Al_{0.12})_2$ system at 4.2 K (Dubenko *et al* 1994a). The solid and dashed lines are the calculated dependences (see text). Inset: the calculated $F(M)/c_7$ dependences for $t = 0, 0.38$ and 1.0.

In order to explain the sudden change of the magnetic properties at t_c Dubenko *et al* (1994a, b) used the Landau expansion for the free energy up to the eighth power of the

magnetization:

$$F(M) = \tfrac{1}{2}c_1M^2 + \tfrac{1}{4}c_3M^4 + \tfrac{1}{6}c_5M^6 + \tfrac{1}{8}c_7M^8 - HM. \tag{24}$$

For a compound with a magnetic ground state and showing IEM $c_1 < 0$, $c_3 > 0$, $c_5 < 0$, $c_7 > 0$ and $F(M)$ has two local minima. The conclusion drawn by the authors was that in the system under consideration there are very small differences in the c_i parameters, and only small changes in their values due to the substitution decide whether WFM or SFM is the ground state. From equation (24) it follows that the two local minima of $F(M)$ reduce to a single one at $t = t_C$.

The quantitative analysis of the $(Y_{1-t}Lu_t)(Co_{0.88}Al_{0.12})_2$ system was performed by Yamada (Dubenko *et al* 1994b). Putting

$$M_2^2 = \tfrac{1}{2}\{M_1^2 + M_3^2\} - \nu(t - t_c) \tag{25}$$

where M_1, M_3 denote the magnetization in the WFM and SFM states, respectively, M_2 is the magnetization at the local maximum of $F(M)$ between $F(M_1)$ and $F(M_3)$ and ν is a positive constant, he has expressed the ratios c_1/c_7, c_3/c_7 and c_5/c_7 as functions of M_1, M_3, ν and t_c. The difference between the two minimum energies at $M = M_1$ and M_3 was then given as

$$\Delta F = -\tfrac{1}{12}c_7\{M_3^2 - M_1^2\}\nu(t - t_c). \tag{26}$$

Assuming $B_M = \Delta F/(M_1 - M_3)$ one gets from equation (26)

$$B_M = -\tfrac{1}{12}c_7\{M_3^2 - M_1^2\}(M_1 + M_3)\nu(t - t_c) \tag{27}$$

where M_1 and M_3 are those at $B = B_M$. The numerical values of c_1, c_3, c_5, c_7 and ν were evaluated from the experimental data on the concentration dependences of M_1, M_3 and B_M (shown in figure 20), the magnetization curve and the high-field susceptibility of $Y(Co_{0.88}Al_{0.12})_2$ (Dubenko *et al* 1994a).

In figure 20, the solid and dashed lines represent the calculated concentration dependences of M_S and B_M, respectively, assuming that the values of c_7 and ν do not depend on t. They are in good agreement with the experimental data. The ratios c_1/c_7 and c_3/c_7 were found to show very weak concentration dependence and c_5/c_7 increased by only about 10% between $t = 0$ and 1. As M_1 is small (0.1 μ_B/fu), the Landau energy and the magnetic equation of state near $M = M_1$ can be given only by the first two terms in equation (24). Therefore M_1 does not depend on concentration. On the other hand, the magnetic characteristics of the SFM state are sensitive to the higher order terms in equation (24).

Assuming now that in $R(Co_{0.88}Al_{0.12})_2$ with magnetic R the local minimum of $F(M)$ at $M = M_3$ is positive, the SFM state in these compounds is stabilized due to the molecular field $B_{RCo}^{(Co)}$. With increasing $B_{RCo}^{(Co)}$, the minimum energy becomes lower and the value of M_3 increases. Based on the $F(M)$ curve of $Y(Co_{0.88}Al_{0.12})_2$, Yamada has shown that the minimum energy calculated for $Tm(Co_{0.88}Al_{0.12})_2$ is higher than that for $Lu(Co_{0.88}Al_{0.12})_2$. This result is consistent with the experimental observation (Dubenko *et al* 1994a).

Khmelevsky and Mohn (2000) performed band structure calculations for YCo_2 for different lattice parameters. It has been shown that IEM exists only for a limited range of the lattice parameter. Changes in the d-band structure among the RCo_2 series, due to the variation of the lattice parameter (following the lanthanide contraction), were found to be the reason why the magnetic transition in $DyCo_2$, $HoCo_2$ and $ErCo_2$ is of a first order type, while it is of a second order type for the remaining RCo_2 compounds.

It is at least plausible that the major differences in the magnetic behaviour of the $Y(Co_{1-x}Al_x)_2$ and the $Lu(Co_{1-x}Al_x)_2$ systems, as discussed above, are due to the difference in the variation of the lattice parameter when substituting Co by Al.

7.2. The $TiCo_2$, $ZrCo_2$ and $HfCo_2$ intermetallics

The compounds with IVA-elements Ti, Zr and Hf crystallize also in the C15 structure. Among them $TiCo_2$ is antiferromagnetic below 43 K (Nakamichi *et al* 1968), while the two other compounds are paramagnets (Oliveira and Harris 1983). The susceptibility of $ZrCo_2$ and $HfCo_2$ obeys a modified Curie law, $\chi = C/(T - T_C) + \chi_0$, with no minimum in χ against T. The electronic specific heat coefficient, γ, is enhanced: 23.3 mJ mol^{-1} K^{-2} and 29 mJ mol^{-1} K^{-2} in $ZrCo_2$ and $HfCo_2$, respectively, if compared e.g. with YNi_2 (Burzo *et al* 1993).

The ρ–T dependences of $ZrCo_2$ and $HfCo_2$ exhibit a much less pronounced saturation tendency than those of YCo_2 and $LuCo_2$ (Baranov *et al* 1993), although they follow a T^2-law at low temperatures. The coefficients A in the $\rho = AT^2$ relation, 0.9 nΩ cm K^{-2} for $ZrCo_2$ and 1.3 nΩ cm K^{-2} for $HfCo_2$; both are much smaller than in YCo_2 and $LuCo_2$ (see section 4). Yamada *et al* (1985) calculated the DOS for $TiCo_2$, $ZrCo_2$ and $HfCo_2$. These calculations revealed that the d–d hybridization in $ZrCo_2$ and $HfCo_2$ is stronger than in YCo_2, $LuCo_2$ and $ScCo_2$. This might explain the difference between the former and the latter group of the Laves phases.

The band calculations of the $Hf(Co_{1-x}Fe_x)_2$ system predict a metamagnetic behaviour in the substituted compounds due to an appropriate shift of ε_f towards lower energies (Yamada and Shimizu 1989). The experimental studies of this system in magnetic fields up to 40 T are qualitatively in agreement with this prediction; the samples with $x = 0.35$, 0.325 and 0.3 show a clear sign of IEM in M against B (Sakakibara *et al* 1988). In contrast to the boundary compound $HfCo_2$, the pseudobinary compounds exhibit a maximum in $\chi(T)$, which is characteristic for IEM. The transitions are however likely of a second order.

The $\rho(T)$ and $S(T)$ dependences of the $Hf(Co_{1-x}Fe_x)_2$ system show that the SF scattering essentially increases when approaching the ferromagnetic instability. In $Hf(Co_{0.7}Fe_{0.3})_2$, the value of is substantially higher compared to that of $HfCo_2$ (Gratz *et al* 1992) and the saturation tendency in $\rho(T)$ is much more pronounced. Similar phenomena were observed in the $Zr(Co_{1-x}Fe_x)_2$ system (Hilscher and Gmelin 1978). An increase of γ up to 64 mJ mol^{-1} K^{-2} for $x = 0.34$ was found. This can obviously be attributed to the increase of SF near the ferromagnetic instability.

8. Conclusion

The procedure used in this paper is based on the comparison of the properties of non-magnetic and magnetic RCo_2 Laves phases. In some cases substitutions either of the Co atoms, e.g. the $Y(Co_{1-x}Al_x)_2$ system, or the R atoms, e.g. $Er_{1-x}Y_xCo_2$, have been used to gain information on the interplay between the Co and the R magnetic sublattices. From this comparison, the conclusion is drawn that there are basically two facts which are behind the large variety of magnetic phenomena for which this family of compounds is known:

(i) There is a hybridization of the 3d band of Co and the 5d band (or 4d band in the case of Y based compounds) of the rare earth element. This follows from the band-structure calculations independent of what method has been used. The field induced magnetic transitions (metamagnetic transition) are closely related to this phenomena.

(ii) The position of the Fermi level in the RCo_2 compounds is located in the vicinity of a steep flank in the energy dependence of DOS. Temperature induced spin fluctuations are thus the consequence, which themselves influence many of the physical properties of these Co based Laves phases. Their influence is most clearly seen in the temperature variation of the transport phenomena, whereas in static measurements such as thermal expansion or magnetostriction their influence is comparatively small.

The theoretical concepts developed due to the investigations of the RCo_2 Laves phases are now widely used to explain magnetic properties of other R–3d intermetallics with lower crystal symmetry and in many cases an even more complicated magnetic behaviour. As examples we will mention the following investigations: (i) The magnetic instability found in YCo_3 (Goto *et al* 1992), (ii) the metamagnetism in the $Ce(Co,Ni)_5$ system (Bartashevich *et al* 1996) and (iii) the magnetic instability observed in the actinide compounds (e.g. UAlCo) (Andreev *et al* 1997).

Finally it should be pointed out that the aspects of magnetic phenomena caused by the R–R interaction only as well as the crystal field effect on the magnetic properties are not considered in this article. These subjects can partly be found in, e.g., Franse and Radwansky (1993) and Gignoux and Schmidt (1995).

Acknowledgments

This work was supported by the Russian Foundation for Basic Research, project number 00-02-17844 and the University of Technology of Vienna, Austria.

References

Aleksandryan V V, Belov K P, Levitin R Z, Markosyan A S and Snegirev V V 1984 *JETP Lett.* **40** 815
Aleksandryan V V, Lagutin A S, Levitin R Z, Markosyan A S and Snegirev V V 1985 *Sov. Phys.–JETP* **62** 153
Aleksandryan V V, Levitin R Z, Markosyan A S, Snegirev V V and Shchurova A D 1987 *Sov. Phys.–JETP* **65** 502
Andreev A V, Bartashevich M I, Goto T, Kamishima K, Havela L and Sechovsky V 1997 *Phys. Rev.* B **55** 5847
Aoki M and Yamada H 1992 *Physica* B **177** 259
Asano S and Ishida S 1987 *J. Magn. Magn. Mater.* **70** 39
Baranov N, Bauer E, Gratz E, Hauser R, Markosyan A S and Resel R 1993 *Int. Conf. on the Physics of Transition Metals* vol II, ed P M Oppeneer and J Kübler (Singapore: World Scientific) p 370
Barron T H K, Collins J G and White G K 1980 *Adv. Phys.* **29** 609
Bartashevich M I, Goto T, Dubenko I S, Kolmakova N P, Kolonogii S A, Levitin R Z and Markosyan A S 1998 *Physica* B **246/247** 487
Bartashevich M I, Goto T, Korolyov A V and Ermolenko A S 1996 *J. Magn. Magn. Mater.* **163** 199
Bloch D, Edwards D M, Shimizu M and Voiron J 1975 *J. Phys. F: Met. Phys.* **5** 1217
Brommer P E, Dubenko I S, Franse J J M, Kayzel F, Kolmakova N P, Levitin R Z, Markosyan A S and Sokolov A Yu 1995 *Physica* B **211** 155
Brommer P E, Dubenko I S, Franse J J M, Levitin R Z, Markosyan A S, Radwanski R J, Snegirev V V and Sokolov A Yu 1993 *Physica* B **183** 363
Burzo E, Gratz E and Pop V 1993 *J. Magn. Magn. Mater.* **123** 159
Burzo E and Lemaire R 1992 *Solid State Commun.* **84** 1145
Coqblin B, Iglesias-Sicardi J R and Jullien R 1978 *Contemp. Phys.* **19** 327
Dubenko I S, Golosovsky I V, Gratz E, Levitin R Z, Markosyan A S, Mirebeau I and Sharygin S V 1995 *J. Magn. Magn. Mater.* **150** 304
Dubenko I S, Kolmakova N P, Levitin R Z, Markosyan A S and Zvezdin A K 1996 *J. Magn. Magn. Mater.* **153** 207
Dubenko I S, Levitin R Z and Markosyan A S 1992 *J. Magn. Magn. Mater.* **111** 146
Dubenko I S, Levitin R Z, Markosyan A S, Snegirev V V and Sokolov A Yu 1994a *J. Magn. Magn. Mater.* **135** 326
Dubenko I S, Levitin R Z, Markosyan A S and Yamada H 1994b *J. Magn. Magn. Mater.* **136** 93
Duc N H and Brommer P E 1999 *Handbook on Magnetic Materials* vol 12, ed K H J Buschow (Amsterdam: Elsevier) ch 3
Duc N H and Goto T 1999 *Handbook on the Physics and Chemistry of Rare Earths* vol 26, ed K A Gschneidner Jr and L Eyring (Amsterdam: Elsevier) ch 171, p 177
Fournier J-M and Gratz E 1993 *Handbook on the Physics and Chemistry of Rare Earths* vol 17, ed K A Gschneidner Jr *et al* (Amsterdam: Elsevier) ch 115, p 409
Franse J J M and Radwanski R J 1993 *Handbook on Magnetic Materials* vol 7, ed K H J Buschow (Amsterdam: Elsevier) ch 5, p 307
Fujii H, Fujimoto J, Takeda S, Hihara T and Okamoto T 1983 *J. Magn. Magn. Mater.* **31–34** 223

Gabelko I L, Levitin R Z, Markosyan A S, Silant'ev V I and Snegirev V V 1991 *J. Magn. Magn. Mater.* **94** 287
Gignoux D and Schmidt D 1995 *Handbook on the Physics and Chemistry of Rare Earths* vol 20, ed K A Gschneidner Jr and L Eyring (Amsterdam: Elsevier) ch 138, p 293
Givord F and Shah J S 1972 *C. R. Acad. Sci., Paris* B **274** 923
Goto T and Bartashevich M I 1999 *J. Phys.: Condens. Matter* **10** 3625
Goto T, Katori H A, Sakakibara T, Mitamura H, Fukamichi K and Murata K 1994a *J. Appl. Phys.* **76** 6682
——1994b *J. Appl. Phys.* **76** 6682
Goto T, Katori H A, Sakakibara T and Yamaguchi M 1992 *Physica* B **177** 225
Goto T, Sakakibara T, Murata K, Komatsu H and Fukamichi K 1990 *J. Magn. Magn. Mater.* **90/91** 700
Gratz E 1997 *Physica* B **237/238** 470
——2001 *Encyclopedia of Materials: Science and Technology* ed K H J Buschow (Amsterdam: Elsevier) section 1.1.9 to be published
Gratz E, Bernhoeft N, Paul-Boncour V, Casalta H and Murani A 2000 *J. Phys.: Condens. Matter* **12** 5507
Gratz E *et al* 1995a *J. Phys.: Condens. Matter* **7** 597
Gratz E and Lindbaum A 1994 *J. Magn. Magn. Mater.* **137** 115
Gratz E, Lindbaum A, Markosyan A S, Mueller H and Sokolov A Yu 1994 *J. Phys.: Condens. Matter* **6** 6699
Gratz E and Nowotny H 1985 *Physica* B **130** 75
Gratz E, Resel R, Bauer E, Pillmayr N and Baranov N 1992 *J. Magn. Magn. Mater.* **104–107** 1918
Gratz E, Resel R, Burkov A T, Bauer E, Markosyan A S and Galatanu A 1995b *J. Phys.: Condens. Matter* **7** 6687
Hauser R, Bauer E, Gratz E, Müller H, Rotter M, Michor H, Hilscher G, Markosyan A S, Kamishima K and Goto T 2000 *Phys. Rev.* B **61** 1198
Hauser R, Kussbach C, Grössinger R, Hilscher G, Arnold Z, Kamarad J, Markosyan A S, Chappel E and Chouteau G 2001 *Physica* B **294/295** 182
Hilscher G and Gmelin E 1978 *J. Physique Coll.* **39** C6 774
Iandelli A and Palenzona A 1979 *Handbook on the Physics and Chemistry of Rare Earths* vol 2, ed K A Gschneidner Jr and L Eyring (Amsterdam: Elsevier) ch 13, p 1
Inoue J and Shimizu M 1988 *J. Phys. F: Met. Phys.* **18** 2487
Khmelevsky S and Mohn P 2000 *J. Phys.: Condens. Matter* **12** 9453
Latroche M, Paul Boncour V, Percheron-Guegan A and Achard J C 1990 *J. Less-Common Met.* **161** L27
Levitin R Z and Markosyan A S 1988 *Sov. Phys.–Usp.* **31** 730
Levitin R Z, Markosyan A S and Snegirev V V 1982 *JETP Lett.* **36** 445
——1984 *Phys. Met. Metallogr.* **57** 36
Markosyan A S and Snegirev V V 1985 *Phys. Met. Metallogr.* **59** 99
Moriya T 1991 *J. Magn. Magn. Mater.* **100** 261
Murata K, Fukamichi K, Goto T, Suzuki K and Sakakibara T 1994 *J. Phys.: Condens. Matter* **6** 6659
Nakamichi T, Aoki Y and Yamamoto M 1968 *J. Phys. Soc. Japan* **25** 77
Oliveira J M C B and Harris I R 1983 *J. Mater. Sci.* **18** 3649
Sakakibara T, Goto T and Nishihara Y 1988 *J. Physique Coll.* **49** C8 263
Sakakibara T, Goto T, Yoshimura K, Shiga M, Nakamura Y and Fukamichi K 1987 *J. Magn. Magn. Mater.* **70** 126
Schwarz K and Mohn P 1984 *J. Phys. F: Met. Phys.* **14** L175
Shimizu M 1981 *Rep. Prog. Phys.* **44** 329
——1982 *J. Physique* **43** 155
Tsuya N, Clark A E and Bozorth R 1964 *Proc. Int. Conf. on Magnetism (Nottingham)* p 250
Tyablikov S V 1965 *Methods of Quantum Theory of Magnetism* (Moscow: Nauka)
Voiron J and Bloch D 1971 *J. Physique* **32** 949
Wada H, Mori T, Shiga M, Aruga Katori H, Bartashevich M I and Goto T 1994 *Physica* B **201** 139
Yamada H 1988 *Physica* B/C **149** 390
——1993 *Phys. Rev.* B **47** 11 211
Yamada H, Inoue J and Shimizu M 1985 *J. Phys. F: Met. Phys.* **15** 169
Yamada H, Inoue J, Terao K, Kanda S and Shimizu M 1984 *J. Phys. F: Met. Phys.* **14** 1943
Yoshimura K and Nakamura Y 1985 *Solid State Commun.* **56** 767
Yoshimura K, Takigawa M, Takahashi Y, Yasuoka H and Nakamura Y 1987 *J. Phys. Soc. Japan* **56** 1138
Ziman J M 1960 *Electrons and Phonons* (Oxford: Oxford University Press)